

**Micro-computed tomography for natural history
specimens:
Handbook of best practice protocols**

Authors:

Kleoniki Keklikoglou (HCMR)

Sarah Faulwetter (HCMR)

Eva Chatzinikolaou (HCMR)

Patricia Wils (MNHN)

Christos Arvanitidis (HCMR)



With contributions from:

Alex Ball (NHM)

Farah Ahmed (NHM)

Laura Tormo (MNCN)

Cristina Paradela (MNCN)



Table of contents

- [1. Scope and structure of this handbook](#)
- [2. The image acquisition workflow](#)
- [3. Protocols for micro-CT image acquisition](#)
 - [3.1 Pre-scan considerations and specimen preparation](#)
 - [3.1.1 Zoological specimens](#)
 - [3.1.2 Botanical specimens](#)
 - [3.1.3 Paleontological specimens](#)
 - [3.1.4 Geological specimens](#)
 - [3.2 Scanning containers and scanning mediums](#)
 - [3.3 Scanning process](#)
 - [3.3.1 Calibrating the system](#)
 - [3.3.2 Placing the specimen](#)
 - [3.3.3 Setting up the detector parameters](#)
 - [3.4. Reconstruction](#)
 - [3.5 Visualisation and post-processing](#)
 - [3.6 Troubleshooting](#)
- [4. Use cases](#)
 - [4.1 Zoological samples](#)
 - [4.2. Botanical samples](#)
 - [4.3. Palaeontological samples](#)
 - [4.4 Geological \(mineral\) samples](#)
- [5. Data curation](#)
 - [5.1 Metadata](#)
 - [5.2 Data organisation, storage and archival](#)
 - [5.3 Data dissemination and publication](#)
- [6. References](#)
- [7. Glossary of terms](#)
- [8. Appendix](#)
 - [8.1 List of institutions with micro-CT](#)
 - [8.2 List of microCT manufacturers](#)
 - [8.3 List of softwares](#)

1. Scope and structure of this handbook

Micro-computed tomography (micro-CT, X-ray computed tomography, high-resolution X-ray computed tomography, HRXCT/HRCT, high resolution CT, X-ray microscopy) is a non-destructive imaging technique which allows the rapid creation of high-resolution three-dimensional data. Based on x-ray imaging, it allows a full virtual representation of both internal and external features of the scanned object. These resulting 3D models can then be either interactively manipulated on screen (rotation, zoom, virtual dissection, isolation of features or organs of interest), or an array of sophisticated 3D measurements can be performed – from simple length and volume measurements to density, porosity, thickness and other material-related parameters.

While having been used in geology and paleontology already for decades (e.g. Carlson & Denison 1992; Simons et al. 1997; Rivers et al. 1999; Sutton et al. 2001; Carlson et al. 2003; Rossi et al. 2004; Burrow et al. 2005; Cnudde et al. 2006; DeVore et al. 2006), in the recent years micro-CT has seen a steep increase of usage in a variety of biological research fields such as taxonomy and systematics, evolutionary and developmental research or functional morphology (see e.g. Faulwetter et al. 2013a and references therein).

The ability of micro-CT imaging to create accurate, virtual representations of both internal and external features of an object, at sub-micron resolution, without destroying the specimen, makes the technique an interesting tool for the digitisation of valuable natural history collections. Digitisation efforts have become an important research activity of museums and herbaria, since collections represent a vast source of biodiversity information which often is underexploited due to the traditionally slow process of re-visiting physical specimens (Blagoderov et al. 2012). Digitised specimens, however, are available at the click of a mouse from any internet-enabled computer worldwide, protect the specimen from loss or damage through handling or shipping and thus have the potential to accelerate taxonomic and systematic research and allow for large-scale comparative morphological studies (Faulwetter et al. 2013a). Micro-CT imaging technology may give rise to the elaboration of “virtual museums” where digital data are shared widely and freely around the world, while the original material is stored safely (Abel et al. 2011). In addition, 3D models created through micro-CT scanning can be either printed or made available via interactive touch screens to be used for public display and outreach efforts.

This handbook acts as a comprehensive guide to micro-CT imaging of different types of natural history specimens, from geological and paleontological to zoological and botanical specimens. First, a general overview of the image acquisition workflow is given, presenting the basic principles of the micro-CT technology. Then, a comprehensive section on best practice protocols follows. For each of the above categories of natural history specimens, a detailed description of best practices, protocols, tips and tricks and use cases are given, from specimen preparation to final use of the resulting models. However, each specimen is different, and each study has a different scope, so naturally there is no standard protocol that can be universally applied. The

information given in this handbook merely acts as a starting point. The last section of the main text comprises information on the data management of the micro-CT datasets, including best practices on metadata, storage and dissemination. Finally, a glossary is included which explains the domain-specific terms used throughout the text, and the appendix includes additional useful information, such as lists of institutions with micro-CT facilities, micro-CT manufacturers and annotated list of softwares.

2. The image acquisition workflow

The basic principle of the micro-CT technique is related to the acquisition of a large set of radiographic projections (2D images) of an object around a rotation axis. The rotated object is placed between an X-ray source and an X-ray detector (Fig. 1) and the free adjustment of the source-object distance (SOD) and object-detector distance (ODD) allows greater resolution in comparison to clinical CT scanners (Schambach et al. 2010).

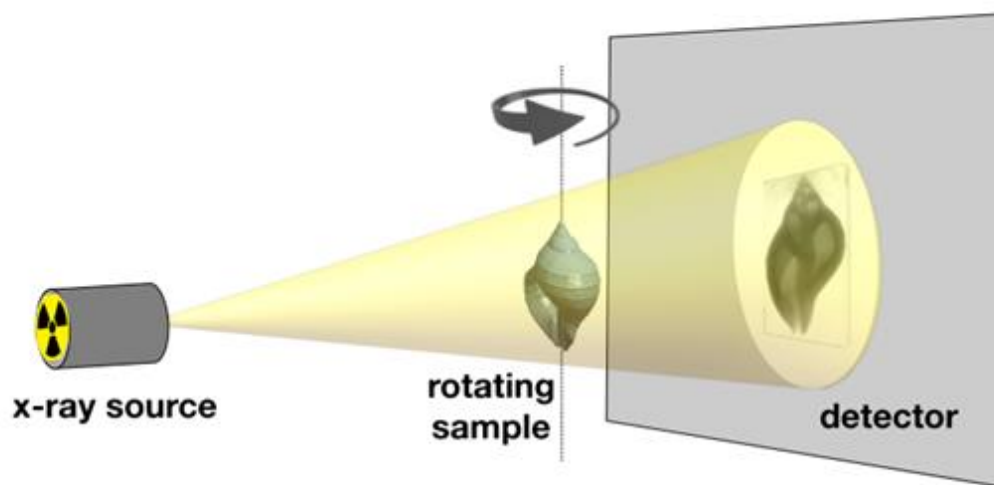


Figure 1. Schematic overview of the image acquisition process. Photos from HCMR micro-CT lab.

The micro-CT technique depends on X-rays which are high energy electromagnetic radiation ranging from hundreds of eV to hundreds of keV. X-rays photons are generated by electron beams. The X-ray source contains an X-ray generator (a vacuum tube) in which electrons are released from a filament (the cathode) and are highly accelerated by an electric potential difference (Fig. 2). Then, the electronic beam is focused on a metal target (the anode) and produce X-rays according to two different processes:

- The electrons are decelerated by the atomic nucleus of the target and their kinetic energy is converted into an emitted X-ray photon. This phenomenon is called 'braking radiation' or Bremsstrahlung. The output spectrum consists of a continuous spectrum of X-rays ranging from 0 to the voltage of the x-ray source.
- The electrons may collide with target orbital electrons and be ejected from the orbit. Subsequently, an electron from a higher energy level will replace the ejected electron and the energy left by this displacement will be transferred to an emitted X-ray photon. The energy of the X-ray photon (fluorescent photon) is the difference between the two energy levels, a characteristic of the target's material.

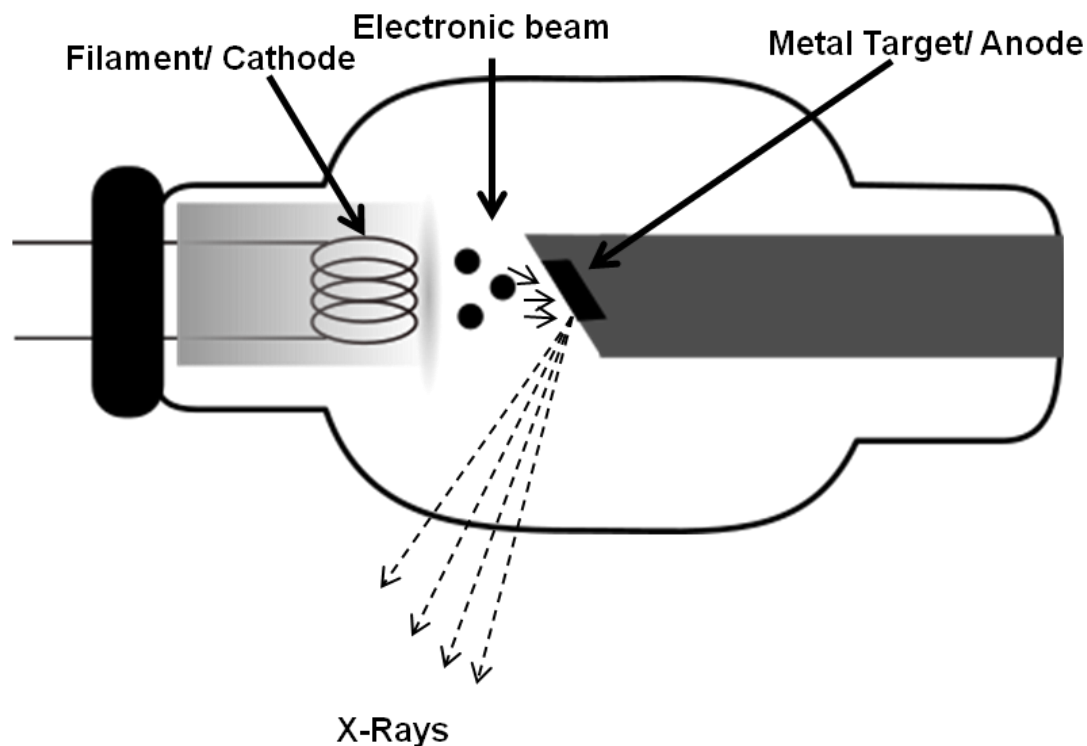


Figure 2. Schematic overview of the X-Ray generator (Modified Image Source: Wikimedia Commons).

The appropriate choice of the target's material aims to ensure that the energy efficiency of the braking radiation is high (its atomic number is high) and the fusion point is high enough to endure high power. Tungsten is used as the main material for high power applications. Another typical material is molybdenum for finer resolution applications. Sutton et al. (2014) has mentioned that a tungsten target source is considered ideal for palaeontological specimens and a molybdenum target source for specimens which are included in amber.

Filters (e.g. aluminium, copper, aluminium and copper combined) can be used to prevent the lowest X-ray photons energy to reach the specimen and to cause artefacts during the reconstruction procedure.

Figure 3 shows a typical spectrum generated by an X-ray generator for 100kV, along with the spectrum when it is filtrated with a 0.5mm copper plate.

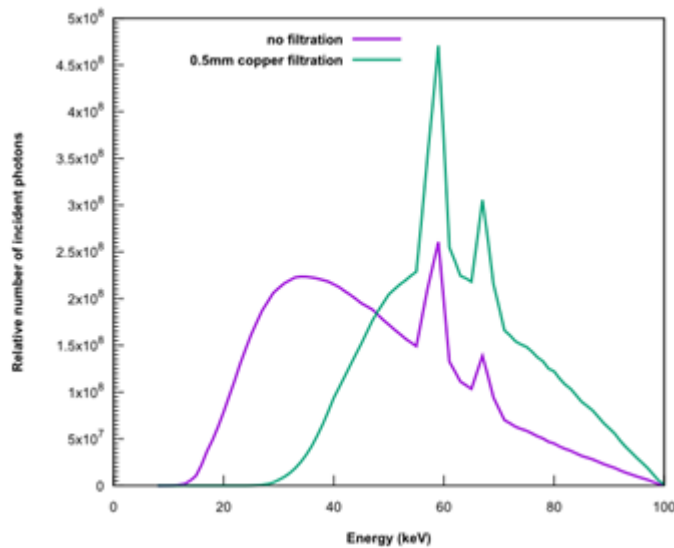


Figure 3. The spectrum generated by an X-ray generator for a 100kV with and without filtration. Photo from MNHN.

X-rays are attenuated along their paths through the specimen due to three types of interactions: photoelectric absorption, Rayleigh scattering and Compton scattering. This attenuation is characterised by a linear coefficient $\mu(E,Z)$ in cm^{-1} that corresponds to the contribution of each type of interaction and depends on the energy of the incident beam and the atomic number of the material encountered.

The total attenuation of an incident beam passing through a well-defined specimen can be computed as a sum or an integration of individual attenuations. This property is a key to tomographic reconstruction, called an inverse problem, as the measurement of the total attenuations on different angles will lead to the knowledge of a discrete set of attenuations (in a voxel grid) along the path through the specimen.

The X-rays photons that have been transmitted through the specimen are then collected on a detection device. A scintillator screen absorbs the X-ray beam and re-emits it in the form of light. This light may be captured by a CCD camera, digitised by a photodiodes array in a flat-panel detector. The choice of a detector is usually a tradeoff between its pixel resolution and its field of view.

The resulting image is a radiograph (projection image) where pixels are coding for the attenuation mapped to 16-bits gray values (ranging from 0 to 65535). This type of acquisition is called absorption-contrast. The darkest parts of an X-ray image are the most absorbing ones

(and their material is of a higher density) and the lightest parts are not absorbing photons (i.e air) (Fig. 4).

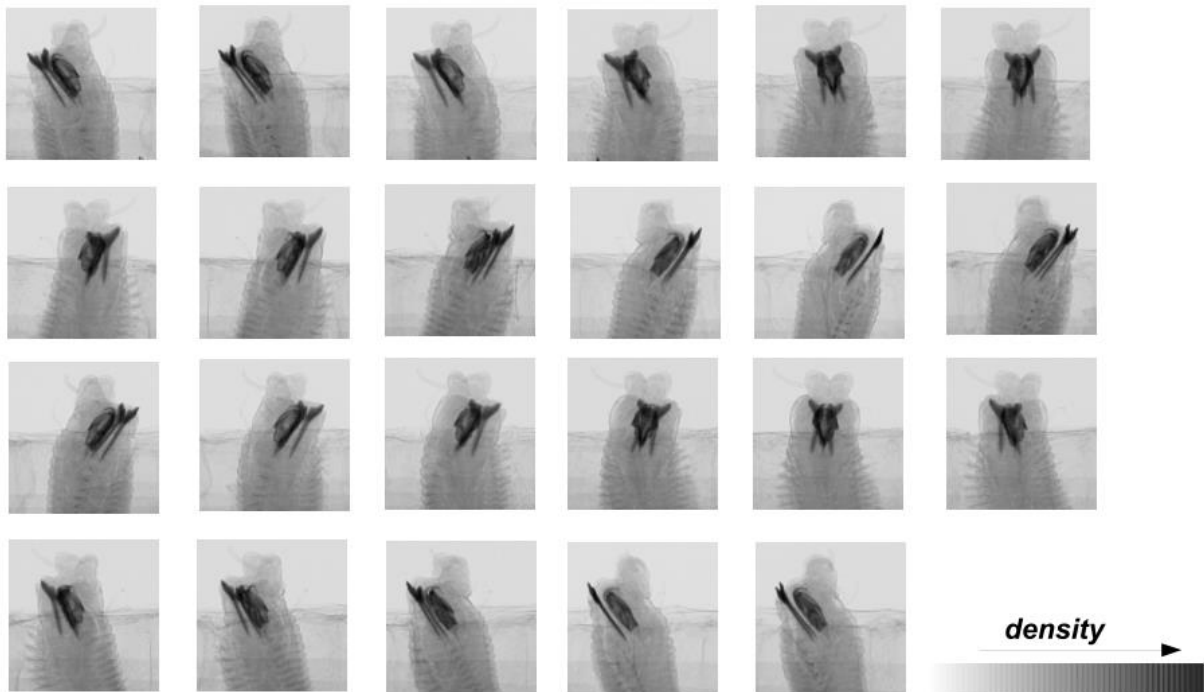


Figure 4. Example for the projection images resulting from the scanning process. Photos from HCMR micro-CT lab.

The aforementioned projection images are reconstructed into cross-section images using specific reconstruction softwares. A reconstruction algorithm is run to get a volumetric representation of the density of the specimen, including its inner features. The most common reconstruction softwares use back-filter algorithms for the recovery of the attenuation maps of the radiographs. Specifically, projection images, which are taken from every angle of the sample, results in sinograms which represents the aforementioned attenuation maps (Betz et al. 2007). The cross-section images (slices) are created by these sinograms using back-filter algorithms. Each projection image is smeared back across the reconstructed image and creates the back-projection images which transmit the measured sinogram back into the image space along the projection paths. The back-projection image is a blurred cross-sectional image. This blurring effect can be moderated using mathematical filters (Sutton et al. 2014) and the algorithms that use the combination of back projection and filtering are known as back-filter algorithms. The combination of the back-projection images will localise the position of the sample. As the number of projections increase, the position and shape of the object becomes more defined (Fig. 5).

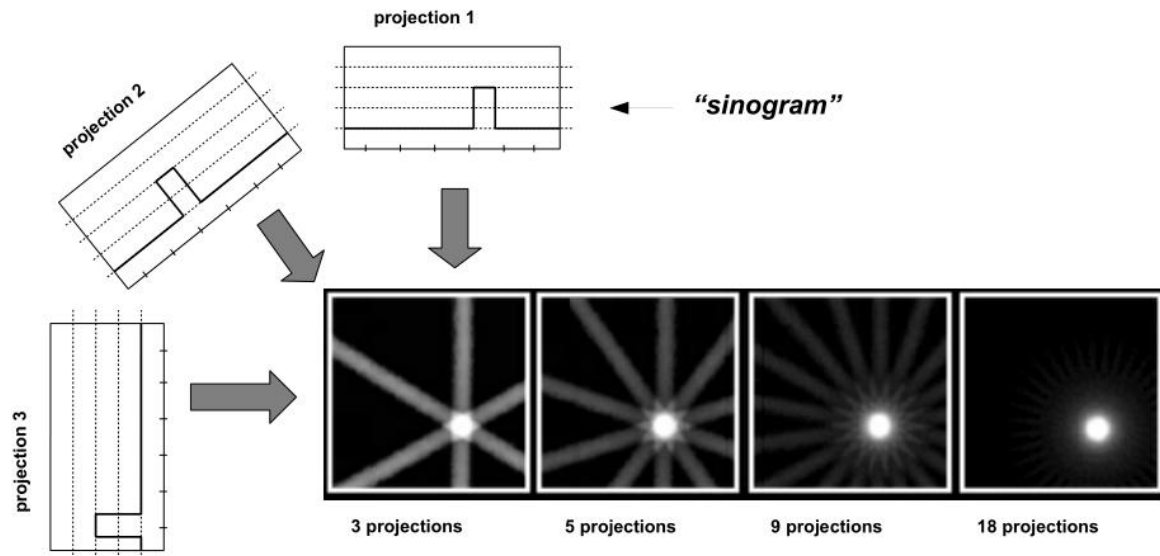


Figure 5. Schematic overview of the reconstruction procedure. Photos from HCMR micro-CT lab.

The reconstruction procedure results in a 3D image where each voxel codes the local density of the specimen. It is usually exported as a stack of 2D images in a given orientation (Fig. 6). The micro-CT dataset can then be processed with dedicated software for 3D visualisation (either through volume rendering or isosurface rendering, see Chapter 3.5) or further analysis (see Chapter 8.3 for a comprehensive list of softwares). The rendered images can be also used for the creation of 3D videos which are an excellent tool for sharing a preview of a micro-CT dataset (Abel et al. 2012).

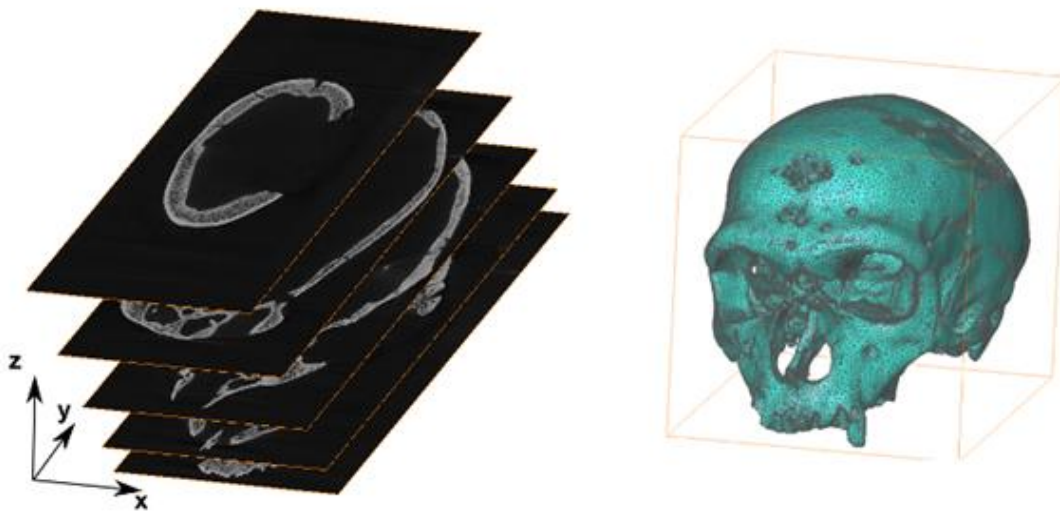


Figure 6. Data processing from a stack of 2D images to a 3D model. Photo from MNHN.

3. Protocols for micro-CT image acquisition

3.1 Pre-scan considerations and specimen preparation

The selection of micro-CT technique as a specimen visualisation method depends on the aim of the specific study. The limitations of the method must be considered, e.g. colour cannot be represented and too tiny structures cannot be detected. An additional consideration when working with museum specimens is to ensure that the museum curator will allow imaging with micro-CT (including contrast enhancement through staining, if needed).

A major point for achieving good results is the contrast difference between the specimen and its surrounding medium. Contrast enhancement agents can be used to improve the quality and clarity of the scanning result: 1) when the specimen has inadequate contrast, 2) when extreme contrast differences between soft and hard tissue need to be reduced (setting of the contrast level in the scan becomes easier), 3) to segment tissues or organs more easily, 4) to identify specific target features of the specimen.

Rehydration or dehydration procedures may be needed before staining, depending on the preservation medium of the specimen or after staining, depending on the medium in which the specimen will be scanned.

3.1.1 Zoological specimens

Dense material, such as bones and other calcified tissues, usually does not require any specific preparation. In soft tissue specimens, where visualisation can be difficult due to the low X-ray absorption of unmineralised tissues (Metscher 2009a; Gignac & Kley 2014), contrast enhancement agents are applied.

A series of the most common contrast agents used in zoological samples is presented in Table 1. In general, contrast agents with a high atomic number are more efficient since they are resulting in an increased difference of X-ray absorption between the stained and unstained tissues (Pauwels et al. 2013). However, the selection of an appropriate and efficient contrast enhancement agent is a combination of several considerations such as the type of the target tissue (see Table 1), the medium in which the specimen was fixed and stored (Metscher, 2009a), the acidity and the penetration rate of the contrast agent (Metscher 2009b; Pauwels et al. 2013; Paterson et al. 2014), as well as the price and toxicity of the staining used. Contrast agents with low penetration rate are more effective when used in relatively small specimens with a sample size of only a few cm³ (Pawels et al. 2013). Staining larger specimens may require longer staining time, as the penetration rate in larger samples may be slower.

Staining of fresh samples will usually give optimal results. However, the results of the staining can be influenced through certain treatments, such as freezing prior to fixation, type or fixation agent, and fixation process (Gignac et al. 2016). If possible, long-term storage in ethanol or unbuffered formalin between fixation and staining should be avoided, as this may affect the morphology of the specimen or alter tissue characteristics which in turn affect staining

properties (e.g. iodine stains bind to lipids, which can be dissolved in alcohols (Gignac et al. 2016), and unbuffered formalin or other acidic liquids may decalcify tissues). However, this is not always possible for museum specimens, and good results have been achieved also with museum specimens stored for years and decades. These finer details of fixative, storage medium, tissue characteristics and staining properties are still insufficiently known and will require further studies in the future.

Micro-CT scanning is a powerful visualisation method with several advantages but might not be appropriate for all kinds of specimens. Some contrast enhancement agents are strong acids (e.g. PTA, PMA, FeCl_3) and when used in high concentrations they may dissolve calcified tissues, such as bones, and destroy the specimen structure (Pauwels et al. 2013). Therefore, in cases where calcified structures are included in the specimen tissue the minimum but still efficient concentration of acidic agents needs to be identified prior staining, or alternatively other non-acidic agents should be used for contrast enhancement.

Contrast agents stored in ethanol (e.g. PTA, iodine) may cause shrinkage when used on specimens which are not stored in ethanol. In such cases a water-based contrast enhancement agent may be more appropriate and safe to use, otherwise a gradual dehydration procedure needs to be followed prior to staining. Shrinkage due to desiccation may destroy the sample and in addition it can create movement artifacts during scanning (Johnson et al. 2011).

Table 1. Overview of the most common contrast agents for soft zoological tissues.

Contrast agent	Tissue	Limitations	Dissolved in	References
Osmium (Osmium tetroxide, OsO_4)	membrane lipids, proteins and nucleic acids	Toxic, volatile, expensive, does not work for tissues preserved in ethanol, slow penetration	phosphate buffer	Metscher 2009b; Kamenz & Weidemann 2009; Faraj et al. 2009
Phosphotungstic acid (PTA)	various proteins (overall structure), connective tissue (collagen), muscle	cartilage matrix does not stain strongly, slow penetration, potential dissolution of calcified tissues if high concentration of contrast agent is used	water or ethanol-methanol	Metscher 2009b; Pauwels et al. 2013
Phosphomolybdic acid (PMA)	cartilage structures, fibrous collagen tissue	slow penetration, potential dissolution of bone structure if high concentration of contrast agent are used	water	Golding & Jones 2007; Pauwels et al. 2013
Iodine	overall structure of soft tissues	may overstain some mineralised tissues	ethanol or methanol	Metscher 2009b; Gignac et al. 2016
Iodine potassium iodide (IKI)	overall structure of soft tissues	may overstain some mineralised tissues	water	Metscher 2009b
Lugol's Iodine (I_2KI)	glycogen, lipids (carbohydrates)	tissue shrinkage at high concentrations, may overstain some mineralised tissues	water	Gignac & Kley 2014

SYNTHEYS3 - Best practice for micro-CT

Gold (Bodian impregnation)	neuron (neuropils)	penetration at 100µm, complex creation of the staining solution	Complex, see Mizutani & Suzuki (2012)	Mizutani & Suzuki 2012; Mizutani et al. 2007
Silver (Golgi silver impregnation)	neuron, cerebral cortex, proteins in polyacrylamide gels, lung tissue	visualisation only 10% of neuron, complex creation of the staining solution	Complex, see Mizutani & Suzuki (2012)	Mizutani & Suzuki 2012; Paterson et al. 2014
Platinum	neuron (substitute of gold)	complex creation of the staining solution	Complex, see Mizutani et al. (2008a,b)	Mizutani et al. 2008a,b
Mercury(II)chloride (HgCl ₂)	cerebral cortex tissue, muscle, fibrous collagen tissue, ligaments, large blood vessels	slow penetration	Complex, see Mizutani et al. (2009)	Pauwels et al. 2013; Mizutani et al. 2009
Lead	muscle, fibrous collagen tissue	precipitations in and around structures	water	Faraj et al. 2009; Pauwels et al. 2013; Kamenz & Weidemann 2009
Barium based (e.g. BaSO ₄ , BaCl ₂)	biofilm in porous media, fibrous collagen tissue	precipitations in and around bone structure	water	Davit et al. 2011; Pauwels et al. 2013
Iron based (e.g. FeCl ₃)	nucleic acids, proteins	slow penetration, dissolution of bone structure	water	Pauwels et al. 2013; Paterson et al. 2014
Hexamethyldisilizane (HMDS)	removes water from tissues, increasing clarity of boundaries between air and tissue	possible internal tissue damage, renders specimens fragile. May react with metal stains previously used on specimen	air	Alba-Tercedor & Sánchez-Tocino 2011; Paterson et al. 2014
Zinc chloride (ZnCl ₂)	muscle, fibrous collagen tissue	slow penetration	water	Pauwels et al. 2013
Ammonium Molybdate Tetrahydrate (NH ₄) ₂ MoO ₄	muscle, fibrous collagen tissue	slow penetration	water	Pauwels et al. 2013
Sodium tungstate (Na ₂ WO ₄)	muscle, fibrous collagen tissue	unknown	water	Pauwels et al. 2013; Kim et al. 2015
Gallocyanin-chromalum	nucleic acids	low overall contrast	water	Presnell et al. 1997; Metscher 2009b

Specimens derived from museum collections need to remain completely intact after their scanning, thus any alterations that might be caused by the staining procedure need to be taken into account. Besides the alterations previously mentioned (decalcification, shrinkage) the

removal of the contrast enhancement agents after scanning is an additional important consideration before using this method on museum specimens. The stability of the stain might depend on the fixation or preservation medium, the age of the specimen, and the type of tissue (e.g. chitin, muscles, calcified tissue) (Schmidbaur et al. 2015). Iodine staining was successfully removed from insects (Alba-Tercedor 2012) and from millipedes (Akkari et al. 2015) by re-immersion into 70% ethanol, and from polychaete tissues using 96% ethanol for 48 hours, while PTA stain was removed using NaOH for 6 hours (Schmidbaur et al. 2015). However, treatment of iodine stained tissues with sodium thiosulfate and of PTA stained tissues with 0.1 M phosphate buffer (pH 8.9) destained the samples even more than their initial unstained status, thus indicating an actual alteration of the tissues characteristics (Schmidbaur et al. 2015). Gignac et al. (2016) also indicated that destaining does not really restore a specimen to its original chemical state, e.g. when iodine stained tissues are treated with sodium thiosulfate, the iodine is transformed to iodide which is colorless and remains in the tissues.

3.1.2 Botanical specimens

Micro-CT scanning of botanical specimens is usually restricted to non-pressed specimens, i.e. those that possess a certain three-dimensional structure. Technically, also pressed herbarium specimens can be scanned under certain circumstances, but the results will likely be of limited research value. Suitable botanical specimens include soft tissues (e.g. flowers, leaves, buds, fruits) and hard tissues (e.g. stems, twigs, roots, nuts). Generally, ligneous hard tissues are more easy to scan than soft tissues, as they do not dry out easily and provide a good contrast due to the higher density of their secondary cell walls. Plant tissues can often be scanned without any need for fixing, preservation of sample, or application of contrast agents. Fruits, nuts, thick roots and wooden structures —and even flowers, if provided with a liquid environment around the stem (van der Niet et al. 2010)— can often simply be scanned fresh without any further preparation. However, if a high resolution of these tissues is required, smaller pieces may be cut from the original sample to decrease the camera-sample distance. Such smaller sample dry out faster and thus may require additional means to prevent dehydration such as wrapping in plastic or parafilm, scanning in a sealed container, or coating the specimen with additional materials (e.g. Korte & Porembski 2011).

Soft tissues are often transparent to X-rays and may require the use of contrast agents, as well as additional preparation to prevent shrinkage during scanning due to desiccation (Stuppy et al. 2003; Leroux et al. 2009). If the sample needs to be fixed and/or stained, a variety of solutions are available. Common fixatives for botanical samples are FAA (formalin - acetic acid - alcohol), formaldehyde, or ethanol (e.g. Leroux et al. 2009; Staedler et al. 2013). However, ethanol has been shown to induce shrinkage in plant tissues and might not be appropriate for all types of studies, e.g. vascular cylinders might be compressed or ruptured if ethanol is used (Leroux et al. 2009).

Samples fixed in a liquid substance will usually require to be scanned in a liquid environment as well, either fully submerged or sealed in a small chamber to prevent drying out. Alternatively,

samples can be embedded in agarose or paraplast, but as this will introduce noise and reduce contrast, these media are only recommended for samples that are either naturally dense or have been treated with heavy-metal stains (see Table 2). Samples can also be critically point dried, freeze-dried or chemically dried with Hexamethyldisilazane (HMDS) and then scanned without any surrounding medium. These methods dry the samples without inducing morphological changes to the tissues, but usually render the sample fragile. The drying can be performed both on stained and unstained samples, but care needs to be taken with HMDS which may chemically react with some stains (e.g. silver stains, see Paterson et al. 2014). Small dried plant samples can also be embedded in a drop of epoxy glue before scanning (Staedler et al. 2013, Fig. 9-F).

A variety of contrast enhancing heavy metal stains has been tested on plant tissues, to varying levels of success and with different tissue specificities. A thorough comparative study has been performed by Staedler et al. (2013). Table 2 summarises the application areas and effects of various heavy metal stains.

Table 2. Overview of the most common contrast agents (heavy metals) for soft botanical tissues.

Contrast agents	Effects- limitations	References
uranyl acetate	Toxic, only slight increase of contrast values compared to other stains.	Leroux et al. 2009 Staedler et al. 2013
iodine	No noticeable contrast increase.	Korte & Porembski 2011 Staedler et al. 2013
potassium permanganate	Permanganate caused visible damage to samples as soon as after 2d infiltration (Fig. 5F), and infiltration for 8 days usually resulted in total sample loss; occasionally increased the contrast of only a part of the sample, leaving other parts unchanged	Staedler et al. 2013
Lugol's solution	causes visible sample damage after several weeks of infiltration.	Staedler et al. 2013
phosphotungstate (PTA)	highest contrast increase on the more cytoplasm- and protein-rich tissues (ovules, ovary wall and pollen)	Staedler et al. 2013
lead citrate	work best on vacuolated tissues (petals, sepals and filaments); highest contrast increase on the more cytoplasm- and protein-rich tissues (ovules, ovary wall and pollen); precipitates in presence of carbon dioxide in the form of lead carbonate crystals [38] that accumulate on the surface of the sample	Staedler et al. 2013
bismuth tartrate	work best on vacuolated tissues (petals, sepals and filaments); highest contrast increase on the more cytoplasm- and protein-rich tissues (ovules, ovary wall and pollen); rendered the samples very delicate and easy to damage	Staedler et al. 2013
osmium tetroxide	work best on vacuolated tissues (petals, sepals and filaments);	Staedler et al. 2013

	highest contrast increase on the more cytoplasm- and protein-rich tissues (ovules, ovary wall and pollen); poor penetration for en-bloc infiltration -> best on open and thin material (open buds, tissues only a few cells thick)	
iron diamine	Samples could not be detected (no increase in contrast)	Staedler et al. 2013

3.1.3 Paleontological specimens

Palaeontological specimens (i.e. fossils) may need to be isolated from rock matrices before scanning in case there is similar X-ray absorption of the specimen and the matrix. Fossils can be extracted from their matrix mechanically by washing, wet sieving and using of several tools such as needles, knives and chisels (Green 2001; Sutton 2008) or chemically, depending on the chemical composition of the surrounding matrix. For example, fossils embedded in calcareous rocks can be isolated using sulphuric acid (Vodrážka 2009) and phosphatic fossils can be extracted using acetic acid (Jeppsson et al. 1999). The maceration procedures of paleontological specimens usually involve physical breakdown, removal of calcareous material, removal of siliceous material, removal of other inorganic material, oxidation, sieving, cleaning and concentrating the organic rich residue (Green 2001). A detailed manual for extraction techniques in palaeontology can be found in Green (2001). However, potential damage of the specimen using chemical extraction methods must be considered (Sutton 2008). If there is no possibility of extraction of the fossil and the contrast between the specimen and the matrix is too low, a synchrotron phase-contrast imaging may be a better solution for the visualisation of such specimens (Sutton 2014).

3.1.4 Geological specimens

Strictly speaking, the only preparation that is absolutely necessary for scanning geological specimens is to ensure that the object fits inside the field of view and that it does not move during the scan (Ketcham & Carlson 2001). Since the full scan field is a cylinder, it is suggested to scan an object of cylindrical geometry, either by using a coring drill to obtain a cylindrical sample of the geological material being scanned, or by packing the object in a cylindrical container with either X-ray-transparent filler or with material of similar density (Ketcham & Carlson 2001).

For some applications the sample can also be treated to enhance the contrasts that are visible. Examples include injecting soils and reservoir rocks with NaI-laced fluids to reveal fluid-flow characteristics (Wellington & Vinegar 1987), injecting sandstones with Woods metal to map out the fine-scale permeability, and soaking samples in water to bring out areas of differing permeability, which can help to reveal fossils (Zinsmeister & De Nooyer 1996).

3.2 Scanning containers and scanning mediums

At the end of the staining procedure, the sample is removed from the solution and washed in distilled water or ethanol (depending on the contrast agent solvent). If specimens are stained or naturally dense they can be scanned in liquid or gel media (water, ethanol, agarose). If they are

stained in air, excess fluid should be blotted away in order to prevent motion artifacts during scanning due to the accumulation of fluid on the bottom of the container (Gignac et al. 2016). Then, the specimen is placed in a sample holder and stabilised in a vertical position for the scanning procedure. The choice of the appropriate sample holder depends on the sample size, the morphology of the specimen and the material from which the sample holder is composed.

Micro-CT companies usually provide a range of several sample holders to the users. It is essential that specimens do not move, settle or wobble during scanning; even a small shift can ruin the image data and necessitate a re-scan (Sutton et al. 2014). Nevertheless, users often create new sample holders according to their needs in order to prevent movement of the specimen during scanning (Figure 7). Glass containers are rarely used since they have a high X-ray absorption, however, glass presents a higher contrast with the background compared to the plastic container, therefore allowing more accurate delineation of the region of interest which corresponds to the inner part of the container (Paquit et al. 2011). Materials such as polypropylene, styrofoam and florist foam have low X-ray absorption, making them ideal as scanning holders. It is also quite common to use pins and clips in order to stabilise the specimen, however, care must be taken in order not to damage museum samples. Sealable plastic bags from which air has been pressed out can be used to prevent drying of specimens (Gignac et al. 2016). Small specimens can be placed in a test tube, an aliquot tube or a micropipette tip (200, 1000, 5000- μ L) (Gignac et al. 2016; Staedler et al. 2013; Metscher 2011) (Fig. 8, 9 B-D). Paraffin wax can be used in the lower end of the pipettes tip as a seal and to stabilise the sample, while Parafilm can be used to seal the upper end of the tip (Staedler et al. 2013, Fig. 9-C). Batch scanning can help to scan large numbers of small samples at the same time and thus decrease overall scanning time: individual samples mounted in pipette tips are mounted in a 1 ml syringe tube and stabilised with resin (Staedler et al. 2013, Fig. 9-D).



Figure 7. Scanning holders: a) fragile Neanderthal bone protected with bubble wrap and fixed in a polystyrene case, b) mammal skulls fixed in a polystyrene case which allows multiple parts to be scanned simultaneously, c) reptilian placed in a polystyrene case; the mouth is kept open using a small piece of polystyrene in order to study the details of the jawbone. Photos from Service of non destructive techniques MNCN-CSIC.

Specimens can be submerged in fluid (e.g. formalin, ethanol or water) during scanning to prevent desiccation (Gignac et al. 2016). Ethanol is less dense than water and provides greater tissue contrast in comparison to water (Metscher 2009a). Scanning small specimens within a liquid medium prevents them from getting stuck on the container's walls. Care must be taken to remove bubbles from the liquid medium in the sample holder as they can create a blurring effect (Metscher 2009a). Agarose can be also used as a scanning medium for small specimens (Metscher 2011). The use of air as a scanning medium gives great results for unstained or dried (e.g. with HMDS) specimens or for studying the internal structure of the specimens. However, scanning in air is not recommended when studying the external morphology of specimens previously immersed in liquid, since the small amount of liquid that will remain on the external surface will be visible as an additional layer in the reconstruction images (Figure 10).

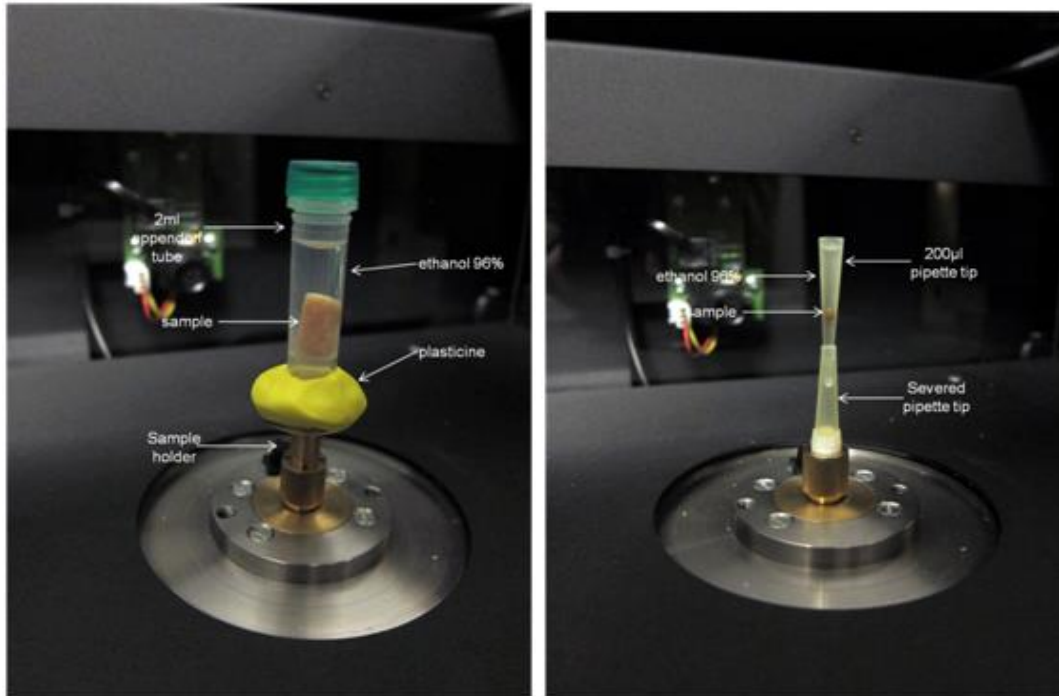


Figure 8. Setup of scanning containers. Photos from HCMR micro-CT lab.

Large plant samples (>10mm) can be mounted in acrylic foam and scanned in a solvent atmosphere, whereas medium sized plant samples are best scanned immersed in the solvent (Staedler et al. 2013). Red and brown algae are easily scanned after having being dried in air. Scanning of the more filamentous green algae and seagrasses within a liquid medium creates artifacts, because their leaves have a low X-ray absorption. Personal experiments showed that staining with PTA or iodine could not improve the resolution. Chemical drying of filamentous algae (e.g. HMDS) and scanning in air can have satisfactory results but due to shrinkage this method is not suggested when aiming to study the internal leaf structure.

Palaeontological specimens are usually scanned in air. However, a celluloid film in organic water-soluble glue is suitable as a scanning medium for isolated microfossils (Görög et al. 2012). Sutton et al. (2014) mentioned that different X-ray penetration between the different axes of a palaeontological sample could cause noise and artifacts and they suggest to bury the specimens in a substance such as flour for low density samples and sand for more dense samples.

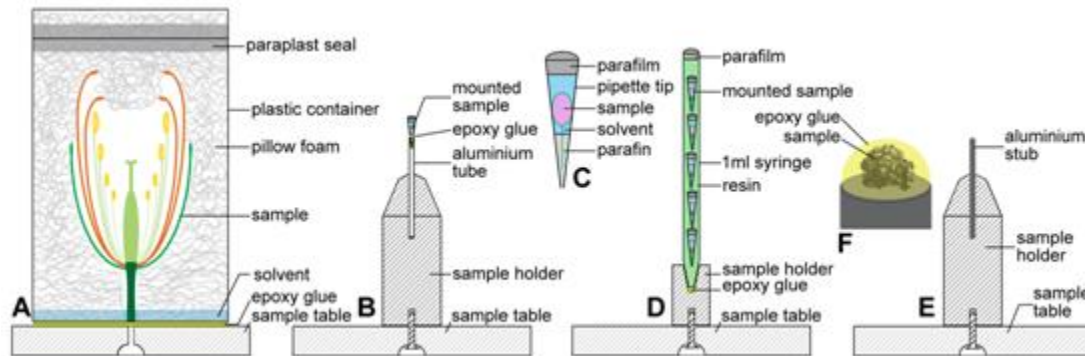


Figure 9. Sample mounting techniques for plant specimens of different sizes. (A) Large samples (>10 mm), (B–D) Medium-sized samples (1–10 mm), (E, F) Small samples (<1 mm). Image from Staedler et al. 2013 (doi:10.1371/journal.pone.0075295.g001).



Figure 10. External morphology of the polychaete *Lumbrineris latreilli*. The remaining ethanol can be observed around the anterior end of the polychaete. Photo from HCMR micro-CT lab.

3.3 Scanning process

Scanning settings differ in terms of voltage, exposure time, magnification and resolution depending on the scope of study, the material of the specimen, the specimen size and the instrument used. A careful balance between all the scanning parameters is necessary to ensure an ideal result and a best practice protocol.

3.3.1 Calibrating the system

In order to achieve a micrometer precision, the incident beam needs to be thin, focused and stable during the acquisition. This calibration of the source includes a software-driven warm-up and focusing. Depending on the scanning system, the user should check the main parameters which are the metal of the source target (if the instrument has this choice), the amount of filtration, the source intensity (in mA) and the source voltage (in kV). The source voltage should be set up in a way that the beam will have sufficient energy to penetrate the specimen and reach the detector. Furthermore, the source intensity should not be too high as the detector may be saturated. On a projection image, the dynamic range (max-min gray value) has to be maximised. A good contrast on the set of projections leads to a good contrast on the final CT image. Too much transmission will reduce the contrast between different densities, while a low transmission will increase the noise level in the images. This contrast issue has to be checked within a complete rotation of the specimen. Adjustment of filter and voltage settings should aim to get a minimum transmission between 10 and 50%.

Scanning of unstained soft tissues usually does not require the use of filters, as they are characterised by a high X-ray transmission. An exception could be a sample which is comprised by a combination of soft and dense structures (e.g. a vertebrate organism), where the use of filter may be helpful. Dense structures, such as bones, shells and other calcified structures, are characterised by a high X-ray absorption, as they contain elements with high atomic number (Schambach et al. 2010). Such structures appear dark on the images and they have low X-ray transmission so the use of filters during scanning is necessary. These filters can be made of aluminium, copper or a combination of the two. Filters reduce artifacts caused from beam hardening effects (Meganck et al. 2009, Abel et al. 2012), while the spread of the X-rays energy distribution is reduced (see Chapter 3.6). However, the use of filters shifts the grayscale values downwards resulting in less contrast between the tissues (Meganck et al. 2009). As already mentioned, increased contrast between the tissues can be achieved by decreasing the voltage, so for dense structures the use of a filter with low voltage will improve the scan.

3.3.2 Placing the specimen

The specimen is placed on a rotating platform between the X-ray source and the detector. It has to be centered vertically and horizontally along the detector. A high-precision rotating mount may help to center small specimens. When acquiring a specific region of interest, this has to be centered instead of the whole specimen. The specimen must not touch either the source or the detector at any time during a complete rotation.

The magnification depends on the distance between the source, the specimen and the detector. The final image voxel size V results from the equation $V = p \times ss/sd$, where p is the detector pixel size, ss the source to specimen distance and sd the source to detector distance. The distances ss and sd may be automatically set by the system or may need a calibration. When the positions of the detector and the rotating platform are set, the calibration usually consists in acquiring a set of radiographs of a calibration object placed on the rotating platform. A greater magnification

and resolution could decrease beam-hardening effects (see Chapter 3.6) but will increase scanning duration. A big specimen size can prevent achieving high magnification and resolution.

3.3.3 Setting up the detector parameters

The calibration of the detector is software-driven (but may need regular initiation by the user) and includes the acquisition of two types of images:

- the dark field image is the resulting image when no X-radiation is emitted. This signal comes from a dark current in the photodiodes of the detector. This image is an offset that will be subtracted from every radiograph.
- the open field images are the response of the detector pixels to the incident beam when no specimen is placed in the system. The software may require a couple of images for different beam intensities or only one for the maximum beam intensity.

In case some pixels are defective, their response will strongly differ from their neighboring ones. When they are detected, a defective map is built and these pixels are ignored during an acquisition. Their values are replaced by an interpolation of the values of non defective neighboring pixels. The defective map should be computed once a month.

Several parameters can usually be changed to influence the imaging process, however, not all scanner models offer the same options. A few important parameters are listed below.

The exposure time E relies on the same principle as the photographic exposure time. It controls the amount of time (in seconds) during which the X-rays will be captured. The detector should collect enough photons at each angle to ensure a good contrast on the radiograph. If the exposure time is very low, projection images will be too dark, contrast will be low and noise in the reconstructed data will be high. High density or thick specimens (e.g. fossils) will need a longer exposure time because fewer photons will be transmitted through them. However, excessively high exposure times may saturate the detector panel (i.e. raise brightness above its maximum measurable threshold). The scanning duration is obviously longer when the exposure times are longer. The use of higher voltage can result in a decrease of the exposure time (Metscher 2009a).

A way to ensure a sufficient contrast without ending up with long scans is to use a binning parameter. Instead of having single cells (or pixels) collecting X-rays on the detector, the signal is acquired using a group of 4 pixels (for a 2*2 binning). The detection is four times higher and there is no need to extend the exposure time anymore. The pixel size and the resulting voxel size are twice bigger. The binning acquisition results in a well-contrasted fast scan but on a lower resolution.

The detector pixels sensitivity is a parameter that helps enhancing a weak X-ray signal when high density or thick specimens almost completely attenuate it.

An averaging parameter A (frame averaging) may be set to improve the image quality. A set of images will be acquired for every angle and only the mean image will be recorded. A higher

number of frames will increase the signal-to-noise ratio. Therefore it is usually recommended to increase the frame averaging for high dense samples when the signal-to-noise ratio is too low.

A pausing parameter P can be used to prevent the afterimage effect. The detector photodiodes need a few ms to get rid of an image. If the acquisition goes too fast, a residual information coming from the previous image may be added to the next image. The pause is used in order to wait for the signal from the previous image to be fully discarded. It may also help to make sure that the specimen is perfectly still after the rotation.

The number N of radiographic images needed to perform a reconstruction can be estimated by measuring the maximum width W of the projected specimen (in pixels) using the formula $N = \pi \times W$ ($\pi=3.14$, Fig. 11) - note that to find the maximum width the specimen should be rotated, as irregularly shaped specimens may have different lengths at different angles. Acquiring less than N projection images will provide an incomplete dataset for the reconstruction algorithm. The reconstruction will be still possible but its quality will be degraded.

The total scanning time T (in seconds) can be computed with the following formula: $T = N \times (P + (E \times A))$.

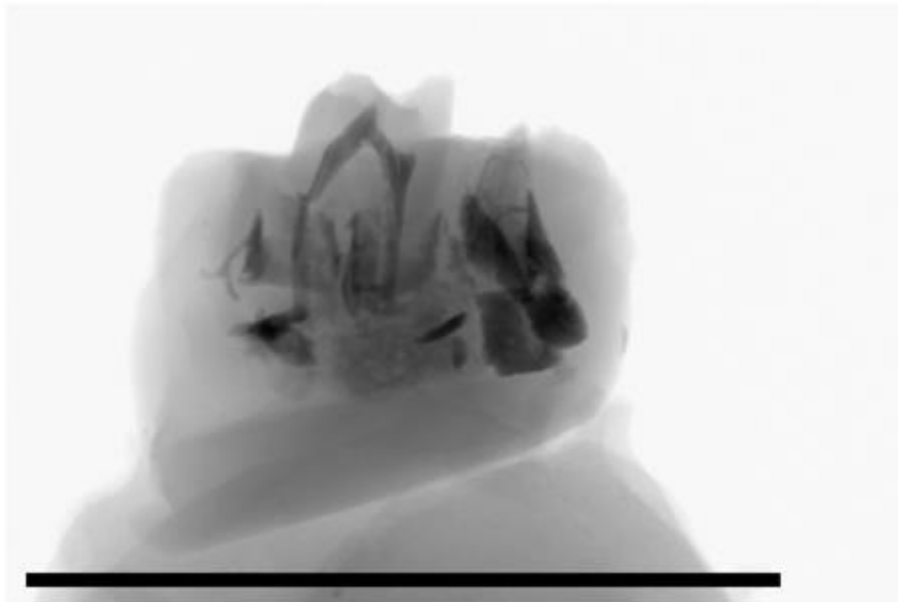


Figure 11. Measuring the maximum width W (in pixels) of the projected specimen (i.e. black line) to calculate the number of radiographs needed. Photo from MNHN.

Other scanning settings include the selection of the rotation step, random movement and 180/360° scan. The selection of an increased rotation step is useful when the scanning duration

needs to be reduced but it can result in images of reduced quality and increased noise. Random movement can be activated to reduce ring artifacts but should not be used when the position of the samples is not secured or when the pixel sizes are very small. The full 360° rotation is selected for scans where the sample consists of a combination of high dense materials inside low dense materials and helps to avoid depletion artifacts. The half (180°) rotation can be used when it is necessary to reduce the scanning time. The simultaneous scan of multiple samples (batch scan) can be used to reduce the overall scanning duration. A short scan duration is beneficiary when specimens are scanned in air and therefore dehydration and shrinkage need to be avoided.

Examples regarding the scanning parameters of zoological, paleontological and geological samples are included in Tables 3–6.

Table 3. Examples of scanning parameters for zoological samples.

Specimen	Voltage (kV)	Current (μ A)	Filter	System	Source	Reference
<i>Alligator mississippiensis</i> (vertebrate)	150-200	130-145	copper	GE phoenix v tome x s240	molybdenum	Gignac & Kley 2014
<i>Dromaius novaehollandiae</i> (vertebrate)	130-180	145-190	copper	GE phoenix v tome x s240	molybdenum	Gignac & Kley, 2014
Polychaeta (invertebrates)	60	167	none	SkyScan 1172	tungsten	Faulwetter et al. 2013a
<i>Apporectodea caliginosa</i> <i>Apporectodea trapezoides</i> (anterior part- invertebrates)	65-70	100	none	Skyscan 1173	tungsten	Fernández et al. 2014

Table 4. Examples of scanning parameters for botanical samples

Specimen	Voltage (kV)	Current (μ A)	Filter	System	Source	Reference
root samples of <i>Asplenium theciferum</i>	50	unknown	none	In-house nano- CT at University of Gent	unknown	Leroux et al. 2009
Xylem of <i>Laurus</i>	50	275	none	Nanotom 180	unknown	Cochard et al.

				XS; GE		2015
macadamia nuts-in-shell	60	unknown	unknown	SkyScan 1172	tungsten	Plougonven et al. 2012
Flower of <i>Bulbophyllum bicoloratum</i>	50	100	unknown	Xradia MicroXCT-200	tungsten	Garmisch et al. 2013

Table 5. Examples of scanning parameters for palaeontological samples.

Specimen	Voltage (kV)	Current (μ A)	Filter	System	Source	Reference
fossils in amber	60	unknown	none	From University of Ghent	unknown	Dierick et al. 2007
fossils in amber	120	unknown	1mm Aluminium	From University of Ghent	unknown	Kehlmaier et al. 2014
<i>Xandarella spectaculum</i> (Arthropoda) in slab	90	120	0.3mm Cu	Phoenix GE Nanotom	tungsten	Liu et al. 2015
Silicified cones	180-200	180-200	unknown	GE Phoenix v tome x s	tungsten	Gee 2013
Ediacara fossil <i>Pteridinium simplex</i>	200	240	none	Ultra-high resolution subsystem of the ACTIS scanner	unknown	Meyer et al. 2014
Trace fossil <i>Trichichnus</i>	130	61	1mm Aluminium	SkyScan 1173	tungsten	Kędzierski et al. 2015
shark tooth of <i>Sphaenacanthus hybodooides</i>	180	138	unknown	Nikon Metrology HMX-ST 225	tungsten	Abel et al. 2012

Table 6. Examples of scanning parameters for geological samples.

Specimen	Voltage (kV)	Current (μ A)	Filter	System	Source	Reference
Meteorite	120–160	60–100	unknown	Nikon Metrology HMX ST 225	tungsten	Hezel et al. 2013
Meteorite	180	120	unknown	Nikon Metrology HMX ST 225	tungsten	Needham et al. 2013

Meteorite	200 kV	160	unknown	Nikon Metrology HMX ST 225	tungsten	Griffin et al. 2012

3.4. Reconstruction

The reconstruction workflow varies between the different scanning systems as each system usually has its own software and most reconstruction steps are automated (Sutton et al. 2014). However, the setting of some reconstruction parameters is necessary and depends on the scope of the reconstruction and the scanning quality. Depending on the scope of the reconstruction, different histogram values are selected as they represent different densities. Concerning the scanning quality, misalignment during the acquisition, noise and ring artifacts may be corrected or improved through using the appropriate reconstruction parameters.

Prior to the reconstruction procedure, some systems can check the projection images for potential movements during the scanning procedure. The alignment of the projection images may fix these movements. If this kind of movements cannot be corrected through the reconstruction procedure, the scanning process should be repeated.

Following the alignment of the projection images, the reconstruction software creates a histogram with the frequency of the grayscale values (density) of the micro-CT dataset. The specific range of the histogram values can reveal different parts of the organisms (Fig. 12). Generally, the peaks in the histogram values represent different structures concerning the different densities. Dense structures such as bones and shells are represented by higher grayscale values in contrast with soft tissues. The choice of an extended range in the histogram can visualise different structures. The range of the grayscale values should be also taken into consideration in order to avoid noise and to isolate unwanted structures (e.g. sample holder).

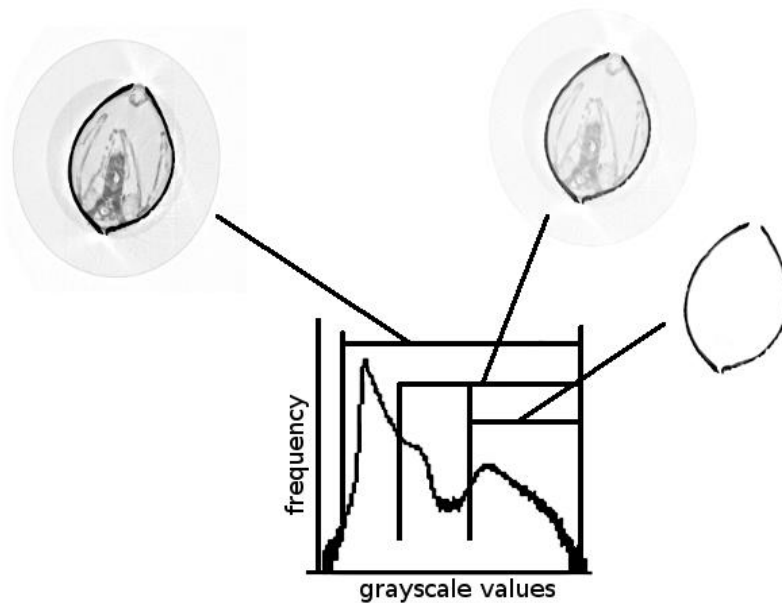


Figure 12. Histogram of the grayscale values frequency of the scanned specimen. Each peak represent different structure of the scanned bivalve.

During the reconstruction procedure, a specific area of the specimen can be reconstructed by creating a region of interest (ROI). For example, the reconstruction of the jaws of a polychaete can be achieved by the creation of a ROI which comprises only these target structures (Fig. 13). This method can minimise the time of the reconstruction procedure, the size of the dataset and the work effort during the dataset processing. The reconstruction duration also depends on the computational resources and capacities, the size of the dataset and the algorithm used (Sutton et al. 2014).

Reconstructed data should ideally be saved without any compression or down-sampling. However, these files will be large, so if storage space is an issue or data should be shared, the creation of compressed image formats (e.g. PNG, JPG) can be considered - always taking into account the detail of information required for the planned analyses. The best lossless image format is TIFF as it can store metadata too (e.g. voxel size, specimen info, scan parameters), however, different systems offer different options.

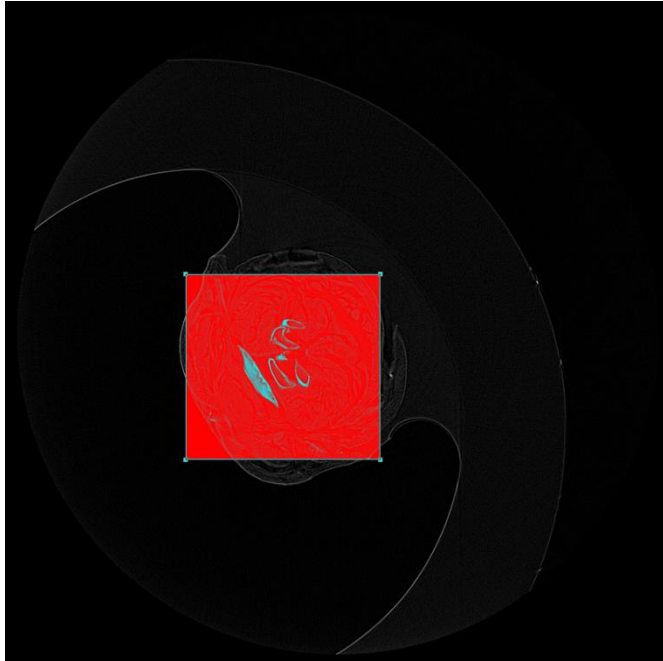


Figure 13. Creation of the region of interest (red square) for the reconstruction of polychaete jaws. Photo from HCMR micro-CT lab.

3.5 Visualisation and post-processing

The reconstructed images can be visualized in 3D using a volume rendering software. A variety of products are available (see Chapter 8.3, Table 8.3.1). The creation of interactive 3D volumes allows the users to explore the dataset from any direction and to manipulate its appearance by changing the rendering parameters (Ruthensteiner et al. 2010). The 3D visualisation of specimens may be used for taxonomic purposes as specific structures can be visualised in their original orientation and shape (see Faulwetter et al. 2013a). A volume can be visualised through volume rendering or through extracting an isosurface (Sutton et al. 2014). Details related to these visualisation methods are presented below.

The post-processing of micro-CT datasets can include simple analyses (e.g. density estimation through the calculation of the grayscale values, porosity, thickness) or advanced morphometric analysis (e.g. geometric morphometrics). The latter requires segmentation of the image (isolation of features of interest and creation of a geometric surface model – see below).

Volume Rendering

The volume rendering procedure assigns colour and opacity to each voxel according to the grayscale values of the sample (Kniss et al. 2002). Some ranges of the histogram can be set to be transparent, mostly to exclude the voxels coding for air or a container. Whenever a structure can be well-defined by its density/gray level on an histogram, it is easily isolated on a volume rendering image by setting everything else transparent (Fig. 14). Advanced rendering

parameters give the user the opportunity to apply false colors and brightness in order to create a realistic rendering.

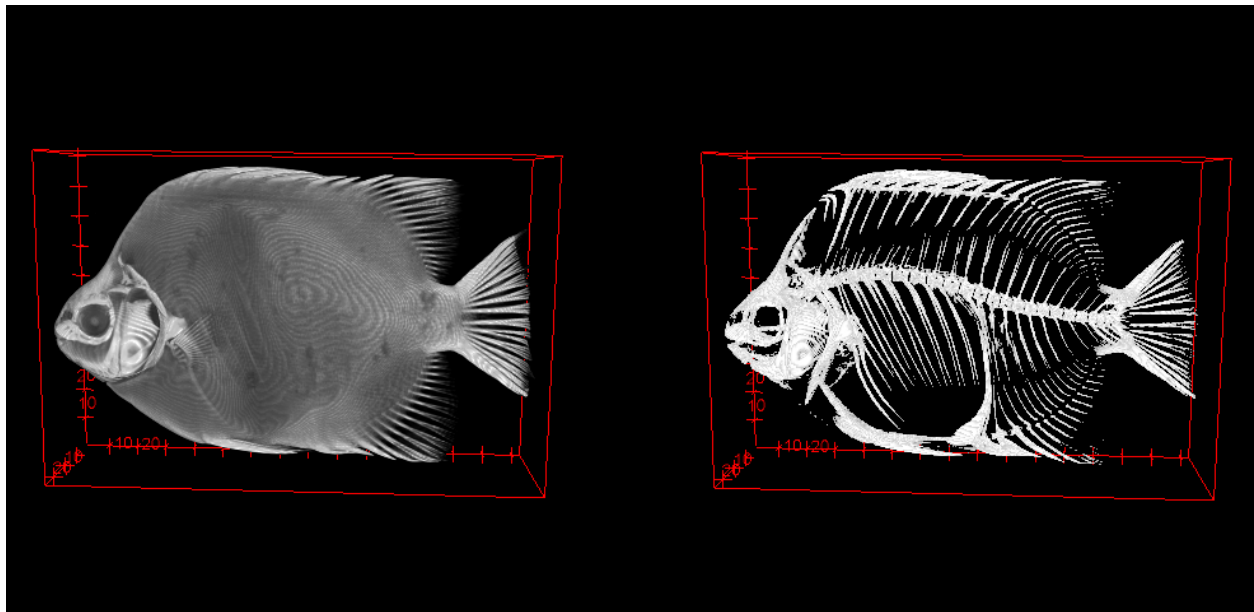


Figure 14. Volume rendering of a specimen where the lowest gray levels coding for air (left) and air+soft tissues (right) are transparent. Photos from MNHN.

Isosurface rendering

An isosurface is a mesh connecting 3D points of a constant intensity within a volume (Fig. 15). The thresholding procedure (or binarisation) of the slices, where the grayscale images are transformed to black and white images, is important for the creation of the 3D model while all voxels are connected above the thresholding value (for softwares see Chapter 8.3, Table 8.3.3.). The 3D model construction is based on the marching cubes algorithm (Lorensen & Cline 1987). The calculation might be time-consuming depending on the size of the data and the computer capacities. The resulting triangle-mesh can be visualised and it is suitable for analysis (e.g. shape analysis, volume, geometric morphometrics. For softwares related to 3D analysis see Chapter 8.3, Table 8.3.4.).



Figure 15. Isosurface rendering of a marine worm (Polychaeta). Photo from HCMR micro-CT lab.

Segmentation

The main drawbacks of volume rendering and isosurface rendering are that neighbouring structures cannot be isolated if their densities are too heterogeneous and their borders not contrasted enough and the user cannot distinguish a specific structure between voxels of similar gray value (for example: visualising only a given bone instead of the whole skeleton, excluding the specimen holder or container). Segmentation is the process of labelling voxels of interest in order to visualise or generate the 3D model of a user-defined structure (Fig. 16). The segmentation procedure can be achieved either manually, semi-automatically or automatically - a large number of algorithms exist for automatic segmentation. Segmentation can be used to include the removal of unwanted objects, to highlight certain structures with colour, or to virtually dissect the sample (Sutton et al. 2014).

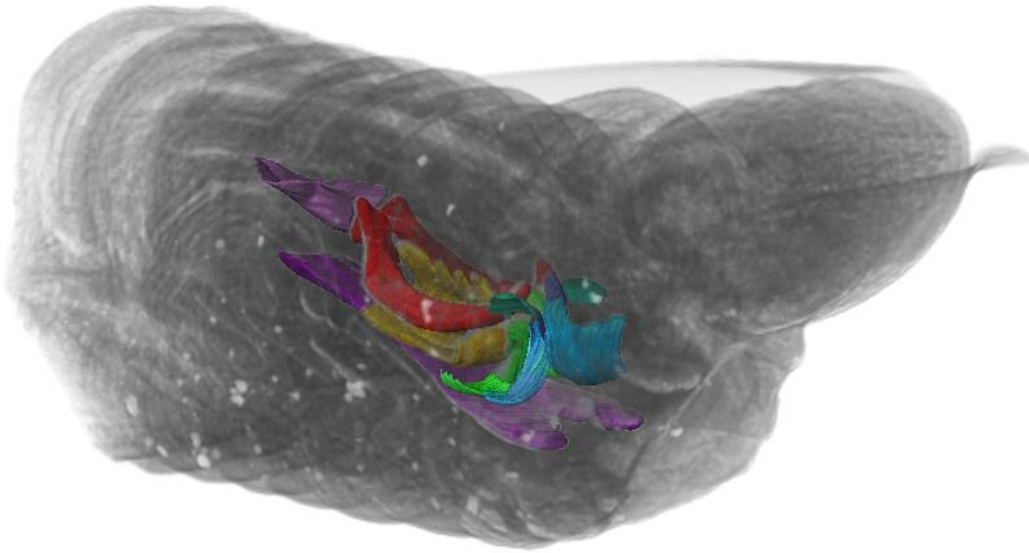


Figure 16. Segmentation of polychaete jaws, highlighting different parts with different colours.
Photo from HCMR micro-CT lab.

3.6 Troubleshooting

Micro-CT scanning is prone to artefacts which can degrade the quality of micro-CT images and the degree of image distortion can make the micro-CT datasets unusable (Barrett & Keat 2004). Artefacts can be created by several processes during the acquisition of micro-CT images. The most common artefacts which are encountered on the micro-CT images are: a) beam hardening artefacts, b) ring artefacts, c) noise, d) partial volume and e) motion artefacts. The avoidance or the correction of these artefacts is important to improve the resulting micro-CT image, but sometimes the effects may be irreversible, so that the scan will have to be repeated.

Beam hardening artefacts

Beam hardening usually occurs when an object consists of different parts with different attenuation coefficients (especially with high densities). This refers to the fact that the beam which penetrates the scanning object becomes harder (increased energy) as the lower energy X-rays are absorbed more rapidly than the higher-energy X-rays (Barrett & Keat 2004). The result of the beam hardening effect is that the object appears to be denser (increased brightness) at the edges than the centre (decreased brightness) creating cupping artefacts (Roche et al. 2010; Abel et al. 2012). A simple approach to solve this problem is to use an X-ray beam of higher energy to ensure that beam hardening is negligible, but this solution is applicable only for small samples (Ketcham & Carlson 2001). Beam hardening effects can also create streaking artefacts which are shown as dark and light streaks around very dense structures. According to Sutton et

al. (2014), the reduction of the streaking artefacts can be achieved by using different scanning media (e.g. water, sand) which act as a filter and smoothen the effect, and through an increase of projection images and a decrease of the exposure time. Beam hardening artefacts can also be minimised by using a metal filter (e.g. aluminum, copper) (Ketcham & Carlson 2001; Barrett & Keat 2004; Meganck et al. 2009; Abel et al. 2012; Sutton et al. 2014), which removes the low energy photons during the scanning procedure. However, this can degrade the X-ray signal to some degree, thus leading to greater image noise unless longer acquisition times are used (Ketcham & Carlson 2001). Concerning cupping artefacts, the use of a combination of aluminum and copper filters is the most effective way for the reduction of these kind of artefacts (Meganck et al. 2009; Hamba et al. 2012). Beam hardening effects can be also reduced to some extent by using the beam hardening correction of the reconstruction software, if provided (Fig. 17).

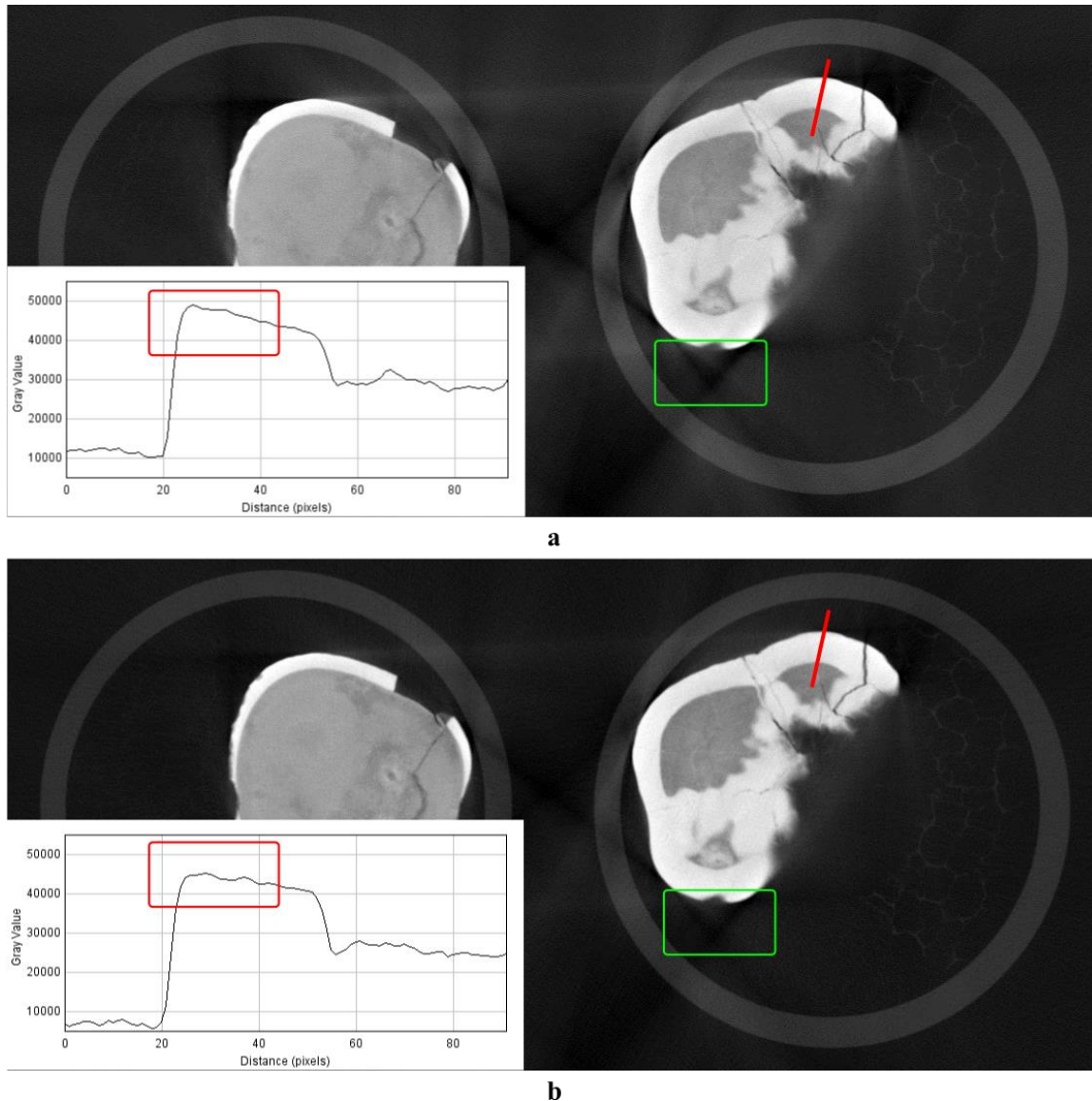


Figure 17. Scan of teeth without (a) and with (b) software beam hardening correction. In red, cupping artefacts increase the reconstructed density at the edges (see plots of gray values along the red lines) and decrease it in the center of the object. In green, streaking artefacts create dark or white lines between structures. Photos from MNHN.

Ring artefacts

Ring artefacts are light and dark rings (circular artefacts) on the reconstructed images (Fig. 18-a) as a result of calibration deficiency of the detector where the X-ray sensitivities of the detector elements are distinguished (Davis & Elliott 1997; Barrett & Keat 2004; Sutton et al. 2014). In some occasions ring artefacts are caused by changes in temperature or beam strength and this can be solved by carefully controlling experimental conditions or by frequent recalibrations (Ketcham & Carlson 2001; Barrett & Keat 2004). The reduction of ring artefacts can be also

achieved through the flat-field corrections (Barrett & Keat 2004; Sutton et al. 2014) and through the selection of the ring artefacts correction during the reconstruction (Fig. 18-b). Furthermore, the selection of the "random movement" option during the scanning procedure could decrease the ring artefacts (Sutton et al. 2014). According to Sutton et al. (2014), if the quality of the micro-CT dataset is significantly decreased by the presence of ring artefacts, the scan should be repeated.

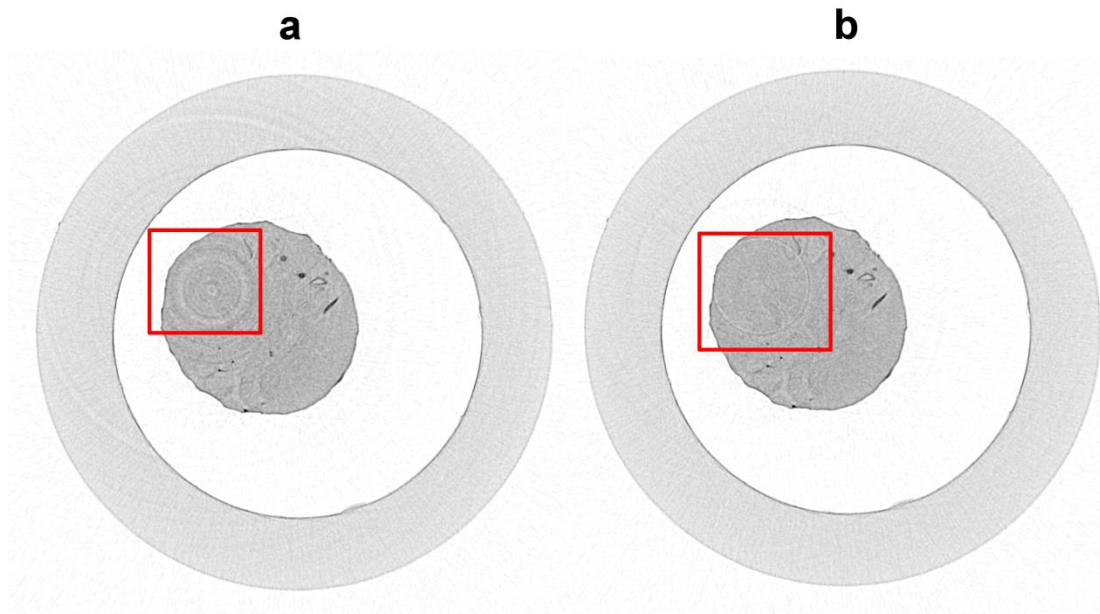


Figure 18. Scan of a marine worm (polychaete) without (a) and (b) with ring artefacts correction during the reconstruction procedure. The red square indicates the presence of ring artefacts which are reduced in (b) following the ring artefacts correction. Photo from HCMR micro-CT lab.

Noise

Noise (or quantum noise) is caused due to statistical error of low photon counts and it is presented as scattered bright and dark streaks in the slices (Fig. 19-a) (Boas & Fleischmann 2012). This kind of artefact can be minimised by using higher beam intensities (increased mAs) which result in better signal-to-noise ratios (SNR) (Boas & Fleischmann 2012; Sutton et al. 2014). Furthermore, an increased source voltage (Kachelrieß 2008; Hsieh 2009; Boas & Fleischmann 2012) and an increased number of projection images (Sutton et al. 2014) may reduce noise. Low exposure times can result in high noise, so increased exposure times and the use of filters may reduce these artefacts in dense samples (Sutton et al. 2014). Furthermore, frame averaging improves the SNR (Sutton et al. 2014). Noise can also be created by physical limitations of the system (e.g. electronic noise in the detector panel) but the reduction of this kind of noise by the operators is difficult (Hsieh 2009). Another factor which contributes to the creation of noise is the reconstruction procedure. The selection of the appropriate reconstruction algorithms and

parameters (e.g. selection of Gaussian filter) can minimise the noise effect (Fig. 19-b) (Hsieh 2009; Sutton et al. 2014).

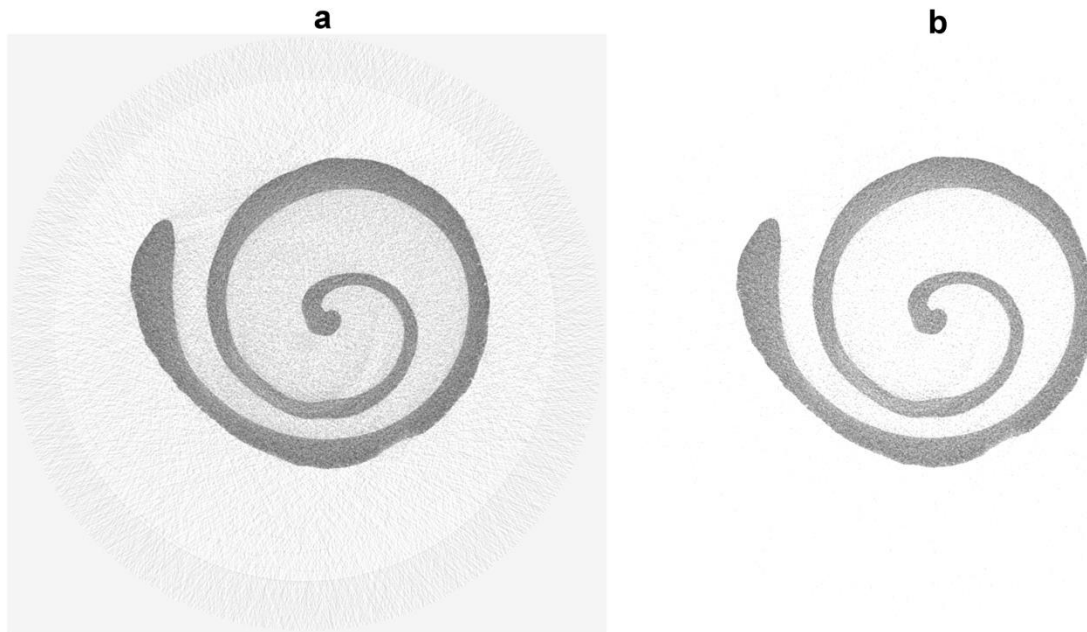


Figure 19. Scan of a bivalve with (a) noise and without (b) noise after the selection of the appropriate parameters during the reconstruction procedure. Photo from HCMR micro-CT lab.

Partial volume

Partial volume effect creates artefacts through the fact that the average attenuation coefficient within a voxel represents an average grayscale value (Barrett & Keat 2004; Abel et al. 2012; Sutton et al. 2014). The result of the aforementioned phenomenon is a gradient, presented as blurring, at the material interfaces (Abel et al. 2012). Sutton et al. (2014) have mentioned that if the anatomical structures are close to the voxel size, then the partial volume effect will be more intense. The use of maximum magnification could decrease the partial volume artefacts but if this effect is remaining, the use of a detector with greater dimensions may be needed (Sutton et al. 2014).

Motion artefacts

Sample motion during the image acquisition creates artefacts which appear as shades or streaks in the reconstructed images (Fig. 20) (Barrett & Keat 2004). Motion artefacts can be reduced through the calculation of the X/Y pixel shifts in the projection images and their correction during the reconstruction procedure (Salmon et al. 2009). However, the prevention of sample movements during the preparation procedure should be taken into consideration as the sample should be stabilised in an appropriate sample holder (see Chapter 3.2). Similar artefacts can also

be created by sample shrinkage where the X/Y correction cannot be performed. The use of a liquid as a scanning medium or the use of parafilm can prevent sample shrinkage and therefore the resulting artefacts.

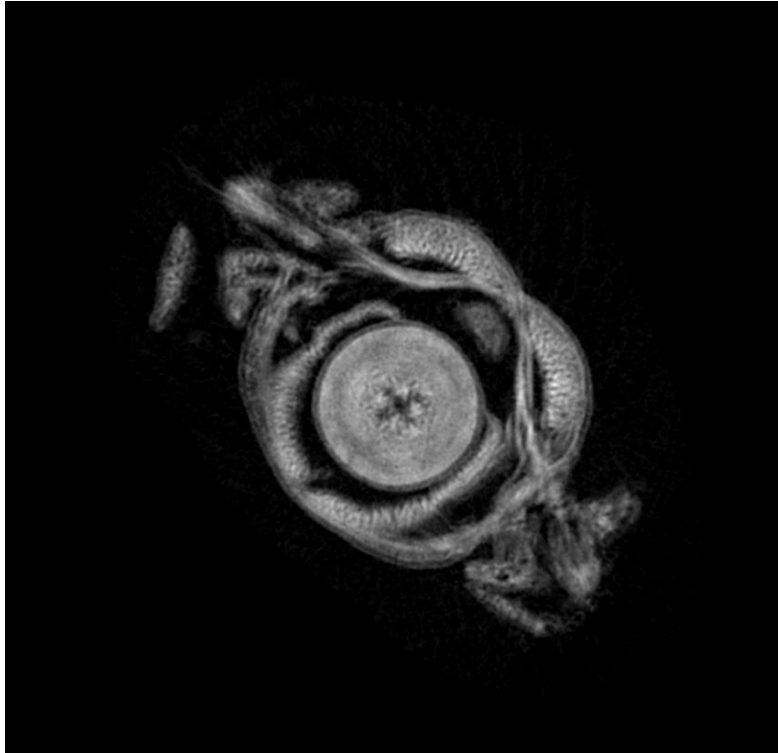


Figure 20. Scan of a marine worm (polychaete) with motion artefacts. The structures are not clearly defined due to specimen movement during the scanning procedure. Photo from HCMR micro-CT lab.

4. Use cases

4.1 Zoological samples

The identification of zoological specimens is usually based on external, internal or on the combination of external and internal morphological characteristics. The 3D nature of the different structures is important for the classification of the organisms (Boistel et al. 2011; Faulwetter et al. 2013a). The creation of 3D models at a resolution of a few microns, the accessibility of micro-CT scanners, the low cost and the use of these datasets for morphometric, functional, ecological and developmental analysis, reveal the utility of this technology for zoological studies (Faulwetter et al. 2013a; Fernández et al. 2014). According to Boistel et al. (2011), different scans –which are referred to as “morphoscans”– should be included into a reliable 3D library with reference models (or gold standards) including intra-species variations and key references established by the community.

Micro-CT is characterised as a non-destructive technology but potential damage on DNA, due to the X-ray radiation, should be considered. Concerning preserved zoological specimens such as museum specimens, studies on the effect of X-rays on bird skins (Paredes et al. 2012) and on invertebrates (Faulwetter et al. 2013a) revealed that exposure to X-rays did not cause damage to the specimen DNA, at least not to the investigated genes. Paredes et al. (2012) speculated that the preservation procedures of the specimen may cause more damages on the DNA quality rather than the X-rays. Similar studies on the effects of the micro-CT technology on the DNA quality of a variety of organisms in different preservation conditions should be carried out before this technology can be safely used on valuable museum specimens (Paredes et al. 2012; Faulwetter et al. 2013a).

Micro-CT technology has been used in morphological and anatomical studies, such as the creation of a 3D interactive model of the jaw musculature of the American Alligator, from which several researchers who are interesting in feeding ecology and evolutionary morphology, have profited (Holliday et al. 2013). Embryonic imaging as well as the quantitative analysis of the organs and tissues of chick embryos has been achieved through micro-CT (Kim et al. 2011) revealing the benefits of this technique for developmental biology (Metscher 2009b; Kim et al. 2011).

Another example of the use of micro-CT in zoological specimens is the assessment of the effects of ocean acidification on calcified structures of marine invertebrates revealing the utility of this technique in ecological studies (Keklikoglou et al. 2015; Chatzinikolaou et al. 2016). Furthermore, Faulwetter et al. (2013a) have proved the benefits of the micro-CT on taxonomical studies through the 3D visualisation of polychaetes.

4.2. Botanical samples

Micro-computed tomography can be still considered as an under-used technique in botanical research (Staedler et al. 2013). Botanical samples often contain soft tissues such as leaves, flowers or fruit tissues with a low x-ray attenuation, and imaging of such parts may require contrast enhancement to increase the quality of images. Best results are usually obtained from samples that consist of different tissue types with different densities, such as seeds, fruits, woods etc, as these allow a better discrimination between individual organs (Leroux et al. 2009). Usually, secondary cell walls are more easily detected than soft tissues (Leroux et al. 2009).

The technique is very suitable for visualising delicate anatomical structures such as embryos, meristems, flowers, and even individual cell walls (Dhondt et al. 2010; van der Niet et al. 2010; Johnson et al. 2011). The applications for micro-CT in botanical research are very diverse. Among the earliest applications of micro-CT in botany were root studies (e.g. Crestana et al. 1986), and literature in this field is abundant (see review of Mooney et al. 2012). Roots, but also whole plants can in many cases also be scanned *in vivo*. This has allowed researchers to perform growth and repair experiments in living studies, and even record time-lapse 3D images (e.g. Brodersen et al. 2010, 2013; Dhondt et al. 2010; Knipfer et al. 2015; Paquit et al. 2014). However, the ionising effect of x-rays has to be taken into account, which may cause growth

inhibition or untypical developments (e.g. Dhondt et al. 2010), so *in vivo* studies need to be planned carefully.

Micro-CT has furthermore been used for morphometric analyses of plants, which form the background for e.g. comparative morphology (Wang et al. 2015; van der Niet et al. 2010), food production (Li et al. 2011) or to address evolutionary questions (Miller & Venable 2003). Due to the high resolution of modern micro-CT scanners– and the large and well-defined cell structures in many plant tissues – cellular structures can often be discerned in plant scans. These fine structures aid in understanding physiological and functional processes in plants (Gamisch et al. 2013, Pajor et al. 2013, McElrone et al. 2013), as cellular architecture profoundly affects the physiology of plant tissues (Pajor et al. 2013). Finally, apart from studying soft plant tissues, micro-CT has been extensively used to study the density and porosity of woods, including plant hydraulics and xylem studies (e.g. Brodersen et al. 2011, Cochard et al. 2015, see also Brodersen & Roddy 2016 for an overview).

4.3. Palaeontological samples

Morphological information on fragile, rare, valuable and extinct palaeontological specimens is accessible through micro-CT technology (Abel et al. 2012). Palaeontological specimens sometimes are included in rock formations or in amber. The investigation of these inclusions using scanning electron microscopy (SEM) or transmission electron microscopy (TEM) provides high quality images but these methods require the destruction of the material (Greco et al. 2011; Görög et al. 2012). The internal information of palaeontological specimens sometimes is important for their taxonomic classification, mostly when their extraction from the rock formations is impossible (Görög et al. 2012). For palaeontological samples, such as the pyritised fossils which are difficult to conserve, micro-CT seems to be the only solution for the visualisation of the internal morphology of the sample, while this technique does not require the removal of the conservation matrix (DeVore et al., 2012). Palaeontological specimens in a rock or amber matrix can be “virtually” extracted using micro-CT (Abel et al. 2012; Konietsko-Meier & Schmitt 2013).

The choice of micro-CT for visualising palaeontological specimens should take into account the required energy that is needed for penetrating such dense samples as well as the required contrast between specimen and matrix (Sutton et al. 2014). Furthermore, the size of the fossils and the size of the structures to be visualised might be an important constraint for the choice of this technology. Micro-CT is suitable for the majority of fossils whose size ranges from 2mm to 200mm (depending on the micro-CT system) due to its energy, scanning parameters and resolution (Sutton et al. 2014). According to Rahman and Smith (2014), micro-CT is suitable for fossil groups such as vertebrates, invertebrates, plants, microfossils, trace fossils and for a variety of their preservation types (including altered preservation, cast, mold, original and permineralisation).

The use of the micro-CT technology in palaeontological collections is mostly related to the 3D visualisation and 3D analysis of palaeontological specimens for taxonomic (e.g. Penney et al.

2007; Briguglio & Benedetti 2012), evolutionary (e.g. Koenigswald et al. 2011; Garwood et al. 2014), histological (e.g. Konietzko-Meier & Schmitt 2013) and palaeoecological purposes (e.g. Wan et al. 2014; Yang et al. 2015). Micro-CT has been used to study the fossil inclusions of amber and this technology revealed features and internal structures which are important for the taxonomical classification of such specimens (Dierick et al. 2007). Furthermore, an example of the utility of micro-CT in morphological and paleobiological studies is the study of the skeleton of an Eocene-Oligocene primate which allowed the visualisation of features related to the life history, locomotion and diet of this primate (Franzen et al. 2009). The digital restoration of the 3D morphology of the Ediacara fossil *Pteridinium simplex* using micro-CT revealed information concerning its ecology and its phylogenetic affinity (Meyer et al. 2014).

4.4 Geological (mineral) samples

Geological applications of X-ray computed tomography include interior examination of one-of-a-kind fossils or meteorites, textural analysis of igneous and metamorphic rocks, geometric description and quantification of porosity and permeability in rocks and soils, and any other application demanding three-dimensional data that formerly required physical serial sectioning (Ketcham & Carlson 2001). Micro-CT scans of rocks are virtual models with gray scale values representing primarily the X-ray attenuation of different minerals or other features, such as pores, in the rock (Wellington and Vinegar 1987). This method offers the means to study the internal materials and geometrics of rare or valuable specimens, such as meteorites, fossils or archaeological artifacts, which should not be destructively sectioned. Even in cases where sectioning is allowed, the use of micro-CT can eliminate the time spent and the laboriousness traditionally faced during the serial sectioning of geological specimens. The digital character of a micro-CT dataset allows interactive manipulation of the data, better visualisation and animation and easier measurement of dimensions (Carlson et. al 2003; Abel et al. 2011).

Micro-CT is a useful tool for the visualization of fractures, pores or layers which are characterised by different densities (Cnudde et al. 2006). According to Stanley (1992) types of rocks that can be examined using micro-CT are:

- igneous rocks formed by the cooling and hardening of molten material (magma), which are composed by interlocking grains, each consisting of a particular mineral).
- rocks formed from sediments (mineral grains) that are deposited at earth's surface by water, ice or air.
- metamorphic rocks formed by the alteration of rocks within the earth under conditions of high temperature and pressure, which are characterised by minerals and textures arrayed in parallel wavy layers.
- crystalline rocks which are igneous and metamorphic rocks formed at high temperatures.

High-resolution X-ray computed tomography has been used to reveal the sizes and the three-dimensional spatial disposition of porphyroblasts in metamorphic rocks, which can indicate the

atomic-scale processes that control crystal nucleation and growth (Denison et al. 1997). Petroleum engineers have used CT data to study two-fluid coreflood experiments in reservoir lithologies (Wellington and Vinegar, 1987). Meteorite investigations have progressed from solely finding inclusions to mapping out the shape and size distributions of their mineralogical components, providing textural clues about their origins (Kuebler et al. 1999). The 3D images produced using micro-CT technology allow the study of the real 3D petrography of meteorites and the visualization of a larger percentage of the meteorite (Hezel et al. 2013).

Another example of the use of micro-CT in petrology studies is the analysis of temporal, geographical and species-specific variations in flaked stone tools morphology which attempts to explain the evolution of cognition, culture and human behaviour. Abel et al. (2011) studied flaked stone tools used by early humans from at least 2.6 million years ago. Using micro-CT, they were able to visualise the key features of percussion, which distinguish flakes intentionally made by humans (artefact) from the ones created naturally (geofact). Also they could recreate missing flakes from refitted groups of material by visualising void spaces (Abel et al. 2011).

5. Data curation

Given the importance of virtual specimens for future research - especially if datasets are designated as cybertypes for species descriptions (see e.g. Akkari et al. 2015) - the data management (or curation) of micro-CT datasets should be performed with the same care as curating physical specimens. Currently, however, there are no universally accepted guidelines or standards concerning the curation, documentation and dissemination of micro-CT datasets. A few general considerations are listed below. These should be taken into consideration by micro-CT laboratories wanting to develop or improve data management practices.

Generally, data management / curation activities can be classified into three broad categories: a) metadata annotation; b) data organization, storage and archival and c) data dissemination.

5.1 Metadata

What is metadata and why is it important?

Metadata is data about data, i.e. information that describes the actual dataset. Metadata serve several purposes:

- a) they help users in discovering and retrieving the dataset according to specific criteria, allowing a user to search / filter for specific attributes;
- b) they help users to gain an overview of the dataset, so that its contents and context can be judged without having to retrieve and explore the actual dataset;
- c) as they make discovery and judging the contents easier, they promote the re-use of data and thus avoid duplication of efforts;

- d) they provide information on the location, accessibility and terms of use of the dataset;
- e) they may document a workflow so that the process of data creation can be understood and repeated; and
- f) they put the dataset in a relationship with other resources, e.g. literature, other datasets, derived information.

Which metadata should be recorded?

The level of detail of the metadata is determined by a variety of factors. Firstly, internal guidelines of the institution, if they exist, may already provide some direction on the type of information that should be recorded along with each dataset. If no institutional guidelines exist, the level of detail needs to be determined by the every-day practices of the laboratory and the demands of the users.

Generally, a balance needs to be sought between the need for a full documentation of the dataset with a high level of detail, and the effort, time and costs required to create this documentation.

As a starting point, the main purpose of the metadata should be determined: are they only needed to accompany the dataset and thus provide a documentation and an overview of the dataset, or is their main purpose to facilitate the discoverability of the dataset? In the former case, a reduced set of core metadata may be sufficient, whereas a higher level of detail with atomised information should be considered to facilitate searching and retrieving the data.

Secondly, the agent creating the metadata needs to be considered to estimate a good balance between effort and level of detail: some metadata can be created automatically by machines (e.g. scanning and reconstruction parameters are usually recorded in a log file by the scanning software; file sizes and number of files in a dataset can be calculated automatically, etc.), whereas others require human efforts (e.g. purpose of the scan, description of specimen, staining protocols, person performing the scan, etc.)

Thirdly, the datasets for which metadata should be created have to be defined: Where do the responsibilities of the micro-CT laboratory lie – are only projection images kept and thus treated as datasets, or should details on reconstructed datasets or other derivative data products also be documented? This will be determined both by institutional policies and daily laboratory practices.

Ideally, a core set of metadata should be developed, which can then be expanded to reflect the needs of the users. Such a core set could, for example, include:

- A unique identifier for the dataset. Ideally, this should be a globally unique identifier, but in case the datasets are used only internally, they can be unique within the lab / institution
- Description of specimen, including a link to an identifier for the specimen e.g. a catalogue number

- Purpose of dataset
- Person(s) involved (for each action, if this level of detail is required)
- Preparations of specimen (e.g. staining) which influence the results
- Date/time of scanning and all scanning parameters (often recorded automatically by the machine)
- Description of / Link to the storage location of the dataset(s)
- Usage restrictions / licenses / copyright
- Information on provenance / changes / version of the dataset (or a “last modified” date)
- Links or identifiers of derived publications or datasets

A defined core set can then be expanded to include additional levels of detail (e.g. information on staining can be recorded in greater detail – which agent, time of staining, person involved; or additional information on the specimen can be included – size, taxonomic classification, preservation medium, age, sex,....), and can also be expanded to describe different parts of the dataset: the set of projection images, the set of reconstructed images, surface models, images and videos, etc.

In which format should metadata be stored? Are there existing standards for describing micro-CT data?

Standards are agreements on how to represent, format and define data – in this case metadata. They are used for ensuring interoperability and comparability between data, and thus are important if data are to be made public, exchanged with others or to be read and processed by specific software packages. As standards are often generic they may not provide the level of detail required for every-day use or analysis of data. For this reason, data are often stored in a more detailed and customised format for internal use which can be mapped and converted to a standard format when the data are to be published or exchanged.

Currently, no metadata standards exist which have been developed specifically for natural history specimens imaged through micro-CT. However, several standards exist that could be adapted to adequately describe these data. The Darwin Core (DwC) format – the predominant format to exchange specimen and occurrence data – is not suitable to adequately describe micro-CT datasets. Although extensions to DwC exist which describe media files (e.g. Simple Multimedia <http://tools.gbif.org/dwca-validator/extension.do?id=gbif; Multimedia> or the Audubon Media Extension <http://rs.tdwg.org/ac/terms/Multimedia>), they cannot represent the information required to describe a micro-CT dataset, in particular information regarding the specimen preparation, scanning and reconstruction process.

A promising standard is the ISA-TAB format (Investigation–Study–Assay; <http://www.isa-tools.org/>; Sansone et al. 2012) which provides flexible options to describe protocols and parameters and to combine metadata terms. It has at least once been applied to document micro-CT data (Akkari et al. 2013), although in a simplified form.

Another option is to use the DICOM format (Digital Imaging and Communications in Medicine; <http://dicom.nema.org>). DICOM is a file format and data exchange protocol extensively used in medical imaging. A DICOM file does not only contain images but also embedded metadata about the imaged specimen (patient, in the case of medical imaging), detailed information on the image acquisition (e.g. type of instrument, settings) and the context of the study. The metadata can be adapted to individual needs, and thus could be tailored towards natural history specimen data. However, DICOM is not straightforward to learn, dedicated software is required, and DICOM is not produced directly by many scanner models, and some software packages require converting DICOM back into image stacks before being able to process the data. Thus, an additional conversion process is often required, which may be cumbersome in the every-day workflow.

How to store metadata?

Generally, there are two ways of storing metadata: embedded in the dataset or external to the dataset (e.g. in a database). Both have advantages and disadvantages:

- Embedded metadata are tied to the data, thus when data are exchanged, metadata automatically are exchanged as well. They are changed along with the data, and thus always reflect the latest changes to the data. However, embedded metadata often do not allow managing and accessing metadata across files and e.g. compare metadata from different files. Thus, embedded metadata are suitable for documenting the data, but less so for enhancing discoverability. DICOM data are an example for embedded data manager, and software exists that facilitates even discovery of metadata across datasets to some extent.
- External metadata are typically stored in a central location, together for all datasets. This allows for efficient search and retrieval of the datasets and enhances discoverability. The metadata can either be submitted along with the dataset (e.g. in a text file) when the data are exchanged, or they can be referenced to it (e.g. if the metadata are available online). However, storing metadata externally may cause inconsistencies between the data and the metadata, if changes are not immediately synchronised. Extensive dissemination and re-publication of the data and metadata may cause different versions of metadata (e.g. licenses) for the same dataset to be produced, causing even more inconsistencies. In addition, the link between data and metadata is a weak one and may be easily lost: if either the metadata are not transferred with the file, or the link to the metadata record is lost, all documentation of the dataset is lost as well.

To decide which system to use for a laboratory, the needs and practices of the institution need to be analysed. If an institutional infrastructure or best practices and guidelines already exist (e.g. an existing database for other imaging systems), the choices will be already limited. If a system is to be set up from scratch, a few considerations may help to determine which system to use:

- *Number of users and central vs. distributed access:* A laboratory with a single user and a single access point (i.e. one PC) will require a less sophisticated system than a laboratory with many users. In a small, single-user lab with a low workload even a well structured and carefully protected single file (e.g. a csv file) might serve, whereas a multi-user lab may want to provide access to the metadata from different PCs and simultaneously. It should also be considered whether the data are made available to users outside the institution, e.g. through a website. In this case, the database needs to be accessible by a web server and protected against attacks.
- *Permissions:* In a multi-user system, different users may have different permissions, e.g. to create new metadata records, to delete records, to edit own records or records of others, or to simply view records. In this case, a user management system needs to be built into the database or software.
- *Purpose of metadata:* Metadata which are mainly used to document the content of the dataset will not require a dedicated and complex system for their storage. If however the main purpose of the metadata is the discovery of datasets through user-defined search criteria, a structured database system with a user interface may be more suitable.
- *Workload:* A high-throughput lab that produces large amounts of metadata may want to invest in a more sophisticated system with more functionality, automated quality controls and multi-user functionality, than a laboratory which infrequently produces new datasets.
- *Availability of IT support:* The complexity of the system will always depend on the extent of IT support that can be provided by the institution. A complex database may need regular IT support, and if that is not available, the performance of the laboratory may be delayed and / or data may get lost.

5.2 Data organisation, storage and archival

File organisation

While careful metadata annotation can help to organise and retrieve the actual datasets, a good file organisation is equally important. Many organisations already have a data organisation framework or guidelines, which can be adopted for micro-CT data. If not, an easy-to-use and consistent system should be developed to systematically store and organise micro-CT data.

Firstly, the lab should decide which data fall under its responsibility. In some laboratories, only the raw data (projection images) are kept, and everything from the reconstructed cross sections to images, analyses and other derivative data falls under the responsibility of the customer / scientist and is not stored or managed by the micro-CT lab. Other practices include to keep the reconstructed set of images too, and certain derivatives (e.g. surface models). A file organisation and storage system should take these responsibilities into account. The structure and names of files will reflect the working practices of the laboratory to some extent, but should take both

usefulness and consistency into account. A structure which can be intuitively and comfortably understood and used by an outsider or by another person a few years into the future is probably a good one. If the lab uses a versioning system, this software may take care of versioning and file organisation, otherwise the file organisation strategy should account for versioning as well.

Some considerations for file organisation:

- Data should be stored in a consistent directory structure. Each directory should have the same internal structure, e.g. for projection data, reconstruction data, surface models, images / videos / analyses, etc – depending on common working practices.
- Folder and file names should be unique and follow a consistent naming scheme. This could contain a unique identifier for the dataset which can be linked to the metadata, or a timestamp (date plus time), or arranged around the instrument, the user or the specimen. Both “talking” file names (names that indicate the content of the dataset) and anonymous file names (e.g. incrementing unique identifiers) have their merits and drawbacks. Talking file names are more intuitive, but unknowingly duplicates may be produced by different users, and they are more difficult to standardise and inconsistencies are introduced more easily. To understand the content of files which are named using identifiers, metadata need to be consulted, but they are easier to organise by an operating system and less prone to duplication and inconsistencies.
- Avoid symbols such as “/ \ : * ? ” < > [] & \$ in file names, as they may have different meanings on different operating systems
- Use underscores (“_”), not spaces to separate parts of filenames, or use CamelCase (noSpacesBetweenWordsAndTheFirstLetterOfEachWordCapitalised)

Storage and archival

Data produced by CT scanners can reach very large file sizes and the disk storage space needed has to be carefully accounted for. Ideally, both the projection data and the reconstructed data should be preserved, especially for specimens that cannot be imaged again (either because they were destroyed during or after the scanning, or because they were lost or are physically decaying). These requirements can be satisfied by enterprise storage systems:

- External and portable hard disks are adequate only for temporarily transporting data. Their use for storing data must be strongly discouraged.
- For online storage and everyday use, enterprise NAS (Network Attached Storage) servers are currently the best option. They can provide scalability and fault tolerance beyond that of discrete hard disks.
- Backups of the online storage should be implemented to ensure data protection. Tape library storage is the most suitable technology for long term storage and currently provide the best capacity to price ratio.

- Off-site storage should be considered as protection against local disasters that might affect both online storage and backups. Cloud storage services can be used to provide this.

5.3 Data dissemination and publication

Data publication

The need to publish and share micro-CT data can stem from different reasons: either it is the general policy of the laboratory to make their data publicly available for re-use, or the data need to be published alongside a scientific publication. If the institution does not host a dedicated file sharing server through which the datasets can be made available, data can be published through a public repository.

Both volumetric datasets (reconstructed images and/or projection images) as well as surface models can be shared and are of interest to the scientific, cultural/artistic and education/science communication community. When sharing data, a suitable licence should be chosen that allow others to re-use and process the data. Creative Commons licenses (<http://www.creativecommons.org>), ideally CC-BY (attribution required) or even CC-Zero (release into the public domain) are the most suitable licenses for sharing scientific data.

The available repositories differ in their scope and features. The choice depends on the type and size of the data to be shared, on whether journal policies apply (e.g. when data accompany a research article), and potentially on institutional practices. An overview of repositories is given in Table 6.

Table 6. Overview of repositories for 3D data.

Data repository	Scope / Restrictions	URL
GigaDB	Accepts almost only data accompanying articles in GigaScience. Data can be however be described as a DataNote and then included in the repository. Focuses on large-size data, i.e. volumetric data. Encourages publication of projection and reconstructed data. All data are released under a CC-Zero waiver (public domain, copyright removed). Assigns DOIs to the data.	http://gigadb.org/
DigitalMorphology	Primarily hosts data from the Digimorph group and collaborators, for contributions the project administrators should be contacted. Available data are QuickTime animations of CT stacks, movies of 3D volume rendering of specimens and STL surface	http://digimorph.org

	models.	
Dryad	Generic data repository. Not tailored towards large files, although they are accepted. Charges a publishing fee (currently \$120 per dataset), unless waivers apply. All data are released under a CC-Zero waiver (public domain, copyright removed). Assigns DOIs to the data.	http://www.datadryad.org
Figshare	Generic data repository. Supports files up to 5GB free (beyond that, institutional services can be purchased). License can be chosen by user. Assigns DOIs to the data.	https://figshare.com
Morphosource	Targeted at 3D biodiversity data (volumetric and surface). File formats include tiff, dicom, stanford ply, and stl. Does not assign DOIs.	http://morphosource.org
MorphDBase	Media database which also develops ontologies that describe morphological terminology. Not specifically targeted at 3D data but accepts media files in general.	https://www.morphdbase.de
Morphomuseum	Publishes data accompanying journal articles in MorphoMuseum, but not only. Focuses on surface models, but volume data can also be published if they accompany surface data. Focus on vertebrates, but does not explicitly exclude other taxa. Assigns DOIs. Only license available is CC-BY-NC.	http://morphomuseum.org
LifewatchGreece micro-CT _{vlab}	Accepts volumetric micro-CT datasets, provides extensive metadata and on-the-fly viewer of volumetric datasets. Several features, e.g. raw data download still under construction. Does not assign DOIs.	https://microct.portal.lifewatchgreece.eu

Tools for outreach and interaction with 3D data

Apart from making 3D datasets available for download, tools exist for remote on-the-fly interaction of users with the data. These tools are useful for giving users an overview of the data without having to download them first, and/or provide a suitable tool for outreach and education.

Surface models can easily be rendered in a browser and allow the user to interact (rotate, zoom, change colours or lights) with them, and multiple technological solutions and ready-made portals exist (e.g. WebGL, Java, Flash). Rendering volumetric data online is still a challenge, and solutions are limited. Arivis Web View (<https://www.arivis.com/de/imaging-science/arivis-webview>) is a commercial solution and provides online 2D and 3D rendering even via limited bandwidth. Drishti Voluminous (<http://voluminous.nci.org.au/homepage>) provides an online version of the volume rendering software Drishti, but is currently only available as a fixed

installation at the National Computational Infrastructure of Australia, which can hosts data upon request. 3D slicer (<https://www.slicer.org/>) is a free software which likewise allows online rendering of volume data, with a variety of features to control opacity and colouring.

In addition to browser-based tools, several applications for mobile phones exist as well (eg. the free CTVOX app, <http://bruker-microct.com/products/ctvox.htm>; ImageVis3D, <http://www.sci.utah.edu/cibc-software/imagevis3d.html>; Volumize, <http://www.volumize.be/>; or DroidRender <https://www.facebook.com/droidrender>). As a rule, these applications will, however, not work on the full high-resolution dataset, but on a downscaled version, as neither memory nor graphics cards on mobile devices are as powerful as those on dedicated desktop computers.

Another tool for interaction with 3D data, and especially for exhibitions, are touch-screen based volume rendering software packages which provide a simplified user interface, allowing children and non-technical users to explore 3D datasets. A commercial solution is the InsideExplorer (<http://www.interspectral.com/inside-explorer/>), which provides also support in setting up exhibitions. Similar features, but without technical support, are provided by the DrishtiPrayog software (<http://nci.org.au/systems-services/scientific-visualisation/visualisation-services/drishti-prayog/>).

Acknowledgments

The authors would like to thank all the SYNTHESYS participants for their contribution to this handbook. This handbook was created under the SYNTHESYS3 project for the deliverable D4.4 - *Protocols for optimal microCT-* (WP4, Obj. 2, Task 2.2).

6. References

- Abel, R. L., Parfitt, S., Ashton, N., Lewis, S. G., Scott, B., & Stringer, C. (2011). Digital preservation and dissemination of ancient lithic technology with modern micro-CT. *Computers & Graphics*, 35(4), 878-884. doi:10.1016/j.cag.2011.03.001
- Abel, R. L., Laurini, C. R., & Richter, M. (2012). A palaeobiologist's guide to 'virtual' micro-CT preparation. *Palaeontologia Electronica*, 15(2), 6T.
- Akkari, N., Enghoff, H., & Metscher, B.D. (2015). A New Dimension in Documenting New Species: High-Detail Imaging for Myriapod Taxonomy and First 3D Cyber-type of a New Millipede Species (Diplopoda, Julida, Julidae). *PLoS ONE* 10(8), e0135243. doi:10.1371/journal.pone.0135243
- Akkari, N., Hostens, J., Weigand, A.M., Zhou, X., Stoev, P., Komerički, A., Liu, S., Porco, D., Penev, L., (2013). Transcriptomic, DNA barcoding, and micro-CT imaging data from an advanced taxonomic description of a novel centipede species (*Eupolybothrus cavernicolus* Komerički & Stoev, sp. n.); *GigaScience*. doi:10.5524/100063
- Alba-Tercedor, J. (2012). Studying the anatomy of wet specimens of mayflies of the genus *Baetis* (Insecta: Ephemeroptera) by scanning them into a liquid with the Skyscan 1172 high resolution micro-CT. Sky Scan MicroCT User Meeting 2012 Abstract Book, 192–195.
- Alba-Tercedor, J., Sánchez-Tocino, L. (2011). The use of the SkyScan 1172 high-resolution micro-CT to elucidate if the spicules of the "sea slugs" (Mollusca: Nudibranchia, Opisthobranchia) have a structural or a defensive function. Sky Scan MicroCT User Meeting 2011 Abstract Book, 113–121.
- Barrett, J. F., & Keat, N. (2004). Artifacts in CT: recognition and avoidance 1. *Radiographics*, 24(6), 1679-1691. doi:10.1148/rg.246045065
- Betz, O., Wegst, U., Weide, D., Heethoff, M., Helfen, L., LEE, W. K., & Cloetens, P. (2007). Imaging applications of synchrotron X-ray phase-contrast microtomography in biological morphology and biomaterials science. I. General aspects of the technique and its advantages in the analysis of millimetre-sized arthropod structure. *Journal of Microscopy*, 227(1), 51-71. doi:10.1111/j.1365-2818.2007.01785.x
- Blagoderov V., Kitching I. J., Livermore L., Simonsen T. J., & Smith V. S. (2012). No specimen left behind: industrial scale digitization of natural history collections. *ZooKeys* 209, 133–146. doi:10.3897/zookeys.209.3178
- Boas, F. E., & Fleischmann, D. (2012). CT artifacts: causes and reduction techniques. *Imaging in Medicine*, 4(2), 229-240. doi:10.2217/iim.12.13

Boistel, R., Swoger, J., Kržič, U., Fernandez, V., Gillet, B., & Reynaud, E. G. (2011). The future of three-dimensional microscopic imaging in marine biology. *Marine Ecology*, 32(4), 438-452. doi:10.1111/j.1439-0485.2011.00442.x

Briguglio, A., & Benedetti, A. (2012). X-ray microtomography as a tool to present and discuss new taxa: the example of *Risananeiza* sp. from the late Chattian of Porto Badisco. *Rendiconti Online Società Geologica Italiana*, 21, 1072-1074.

Brodersen, C. R., McElrone, A. J., Choat, B., Matthews, M. A. & Shackel, K. A. (2010). The dynamics of embolism repair in xylem: In vivo visualizations using high-resolution computed tomography. *Plant Physiology*, 154, 1088–1095. doi:10.1104/pp.110.162396

Brodersen, C.R., Lee, E. F., Choat, B., Jansen, S., Phillips, R. J., Shackel, K. A., McElrone, A. J. & Matthews, M. A. (2011). Automated analysis of three-dimensional xylem networks using high-resolution computed tomography. *The New Phytologist*, 191, 1168–1179. doi:10.1111/j.1469-8137.2011.03754.x

Brodersen, C. R., McElrone, A. J., Choat, B., Lee, E. F., Shackel, K. A. & Matthews, M. A. (2013). In vivo visualizations of drought-induced embolism spread in *Vitis vinifera*. *Plant Physiology*, 161, 1820–1829. doi:10.1104/pp.112.212712

Brodersen, C.R. & Roddy, A. B. (2016). New frontiers in the three-dimensional visualization of plant structure and function. *American Journal of Botany*, 103, 1–5. doi:10.3732/ajb.1500532

Burrow, C. J., Jones, A. S., & Young, G. C. (2005). X-ray microtomography of 410 million-year-old optic capsules from placoderm fishes. *Micron*, 36(6), 551-557. doi:10.1016/j.micron.2005.05.005

Carlson, W. D., & Denison, C. (1992). Mechanisms of porphyroblast crystallization: results from high-resolution computed X-ray tomography. *Science*, 257(5074), 1236-1239.

Carlson, W.D., Rowe, T., Ketcham, R.A., & Colbert, M.W. (2003). Applications of high-resolution X-ray computed tomography in petrology, meteoritics and palaeontology. In: Applications of V-ray Computed Tomography in the Geosciences (Eds. Mees F, Swennen R, Van Geet M, Jacobs P). *Geological Society, London, Special Publications*, 215(1), 7-22.

Chatzinikolaou, E., Grigoriou P., Keklikoglou, K., Faulwetter, S., & Papageorgiou, N. (2016, submitted). The combined effects of ocean acidification and elevated temperature on the shell density of two gastropod species using micro-CT imaging. *ICES Journal of Marine Science*.

Cnudde, V., Masschaele, B., Dierick, M., Vlassenbroeck, J., Van Hoorebeke, L., & Jacobs, P. (2006). Recent progress in X-ray CT as a geosciences tool. *Applied Geochemistry*, 21(5), 826-832. doi:10.1016/j.apgeochem.2006.02.010

Cochard, H., Delzon, S. & Badel, E. (2015). X-ray microtomography (micro-CT): A reference technology for high-resolution quantification of xylem embolism in trees. *Plant, Cell and Environment*, 38(1), 201-206. doi:10.1111/pce.12391

Crestana, S., Cesaero, R. & Mascarenhas, S. (1986). Using a computer assisted tomography miniscanner in soil science. *Soil Science*, 142, 56–61

Davis, G. R., & Elliott, J. C. (1997). X-ray microtomography scanner using time-delay integration for elimination of ring artefacts in the reconstructed image. *Nuclear Instruments and Methods in Physics Research Section A: Accelerators, Spectrometers, Detectors and Associated Equipment*, 394(1), 157-162. doi:10.1016/S0168-9002(97)00566-4

Davit, Y., Iltis, G., Debenest, G., Veran-Tissoires S., Wildenschild, D., Gérino, M., & Quintard, M. (2011). Imaging biofilm in porous media using X-ray computed microtomography. *Journal of microscopy*, 242(1), 15-25. doi:10.1111/j.1365-2818.2010.03432.x

Denison, C., Carlson, W. D., Ketcham, R. A. (1997). Three-dimensional quantitative textural analysis of metamorphic rocks using high-resolution computed X-ray tomography: Part I. Methods and techniques. *Journal of Metamorphic Geology*, 15(1), 29–44. doi:10.1111/j.1525-1314.1997.00006.x

DeVore, M. L., Kenrick, P., Pigg, K. B., & Ketcham, R. A. (2006). Utility of high resolution x-ray computed tomography (HRXCT) for paleobotanical studies: an example using London Clay fruits and seeds. *American Journal of Botany*, 93(12), 1848-1851.

Dhondt, S., Vanhaeren, H., Van Loo, D., Cnudde, V. & Inzé, D. (2010). Plant structure visualization by high-resolution X-ray computed tomography. *Trends in Plant Science*, 15, 419–422. doi:10.1016/j.tplants.2010.05.002

Dierick, M., Cnudde, V., Masschaele, B., Vlassenbroeck, J., Van Hoorebeke, L., & Jacobs, P. (2007). Micro-CT of fossils preserved in amber. *Nuclear Instruments and Methods in Physics Research Section A: Accelerators, Spectrometers, Detectors and Associated Equipment*, 580(1), 641-643. doi:10.1016/j.nima.2007.05.030

Elangovan, P., Hezel, D. C., Howard, L., Armstrong, R., & Abel, R. L. (2012). PhaseQuant: A tool for quantifying tomographic data sets of geological specimens. *Computers & Geosciences*, 48, 323-329. doi:10.1016/j.cageo.2012.01.014

Faraj, K. A., Cuijpers, V. M., Wismans, R. G., Walboomers, X. F., Jansen, J. A., van Kuppevelt, T. H., & Daamen, W. F. (2009). Micro-computed tomographical imaging of soft biological materials using contrast techniques. *Tissue Engineering Part C: Methods*, 15(3), 493-499. doi:10.1089/ten.tec.2008.0436.

Faulwetter, S., Vasileiadou, A., Kouratoras, M., Dailianis, T., & Arvanitidis, C. (2013a). Micro-computed tomography: Introducing new dimensions to taxonomy. *ZooKeys*, 263: 1-45. doi:10.3897/zookeys.263.4261

Faulwetter, S., Dailianis, T., Vasileiadou, A., & Arvanitidis, C. (2013b). Contrast enhancing techniques for the application of micro-CT in marine biodiversity studies. *Microscopy and Analysis*, 27(2), S4-S7.

- Fernández, R., Kvist, S., Lenihan, J., Giribet, G., & Ziegler, A. (2014). Sine systemate chaos? A versatile tool for earthworm taxonomy: non-destructive imaging of freshly fixed and museum specimens using micro-computed tomography. *PLoS one*, *9*(5), e96617. doi:10.1371/journal.pone.0096617
- Franzen, J. L., Gingerich, P. D., Habersetzer, J., Hurum, J. H., von Koenigswald, W., & Smith, B. H. (2009). Complete primate skeleton from the middle Eocene of Messel in Germany: morphology and paleobiology. *PLoS one*, *4*(5), e5723. doi:10.1371/journal.pone.0005723
- Friis, E. M., Crane, P. R., Pedersen, K. R., Bengtson, S., Donoghue, P. C., Grimm, G. W., & Stampanoni, M. (2007). Phase-contrast X-ray microtomography links Cretaceous seeds with Gnetales and Bennettitales. *Nature*, *450*(7169), 549-552. doi:10.1038/nature06278
- Gamisch, A., Staedler, Y. M., Schönenberger, J., Fischer, G. A. & Comes, H. P. (2013). Histological and Micro-CT Evidence of Stigmatic Rostellum Receptivity Promoting Auto-Pollination in the Madagascan Orchid *Bulbophyllum bicoloratum*. *PLoS ONE*, *8*(8), e72688. doi:10.1371/journal.pone.0072688
- Garwood, R. J., Sharma, P. P., Dunlop, J. A., & Giribet, G. (2014). A Paleozoic stem group to mite harvestmen revealed through integration of phylogenetics and development. *Current Biology*, *24*(9), 1017-1023. doi:10.1016/j.cub.2014.03.039
- Gee, C. T. (2013). Applying microCT and 3D visualization to Jurassic silicified conifer seed cones: a virtual advantage over thin-sectioning. *Applications in plant sciences*, *1*(11), 1300039. doi:10.3732/apps.1300039
- Gignac, P. M., & Kley, N. J. (2014). Iodine-enhanced micro-CT imaging: Methodological refinements for the study of the soft-tissue anatomy of post-embryonic vertebrates. *Journal of Experimental Zoology Part B: Molecular and Developmental Evolution*, *322*(3), 166-176. doi:10.1002/jez.b.22561
- Gignac, P. M., Kley, N. J., Clarke, J. A., Colbert, M. W., Morhardt, A. C., Cerio, D., Cost, I. N., Cox, P. G., Daza, J. D., Early, C. M., Echols, M. S., Henkelman, R. M., Herdina, A. N., Holliday, C. M., Li, Z., Mahlow, K., Merchant, S., Müller, J., Orsbon, C. P., Paluh, D. J., Thies, M. L., Tsai, H. P., & Witmer, L. M. (2016). Diffusible iodine-based contrast-enhanced computed tomography (diceCT): an emerging tool for rapid, high-resolution, 3-D imaging of metazoan soft tissues. *Journal of anatomy*, *228*(6), 889-909. doi:10.1111/joa.12449
- Golding, R. E., & Jones, A. S. (2007). Micro-CT as a novel technique for 3D reconstruction of molluscan anatomy. *Molluscan Res*, *27*, 123-128.
- Görög, Á., Szinger, B., Tóth, E., & Viskok, J. (2012). Methodology of the micro-computer tomography on foraminifera. *Palaeontologia Electronica*, *15*(1), 15.
- Greco, M. K., Welz, P. M., Siegrist, M., Ferguson, S. J., Gallmann, P., Roubik, D. W., & Engel, M. S. (2011). Description of an ancient social bee trapped in amber using diagnostic radioentomology. *Insectes Sociaux*, *58*(4), 487-494. doi:10.1007/s00040-011-0168-8

Green, O. R. (2001). A manual of practical laboratory and field techniques in palaeobiology. *Springer Science & Business Media*. doi:10.1007/978/94-017-0581-3

Griffin, L. D., Elangovan, P., Mundell, A., & Hezel, D. C. (2012). Improved segmentation of meteorite micro-CT images using local histograms. *Computers & Geosciences*, 39, 129-134. doi:10.1016/j.cageo.2011.07.002

Hamba, H., Nikaido, T., Sadr, A., Nakashima, S., & Tagami, J. (2012). Enamel lesion parameter correlations between polychromatic micro-CT and TMR. *Journal of dental research*, 91(6), 586-591. doi:10.1177/0022034512444127

Hezel, D. C., Elangovan, P., Viehmann, S., Howard, L., Abel, R. L., & Armstrong, R. (2013). Visualisation and quantification of CV chondrite petrography using micro-tomography. *Geochimica et Cosmochimica Acta*, 116, 33-40. doi:10.1016/j.gca.2012.03.015

Hsieh, J. (2009). Computed tomography: principles, design, artifacts, and recent advances. Bellingham, WA: SPIE. doi:10.1117/3.817303

Holliday, C. M., Tsai, H. P., Skiljan, R. J., George, I. D., & Pathan, S. (2013). A 3D interactive model and atlas of the jaw musculature of Alligator mississippiensis. *PloS one*, 8(6), e62806. doi:10.1371/journal.pone.0062806

Jeppsson, L., Anehus, R., & Fredholm, D. (1999). The optimal acetate buffered acetic acid technique for extracting phosphatic fossils. *Journal of Paleontology*, 964-972.

Johnson, E., Dwarthe, D., & Jones, A. (2011). Specimen preparation for X-ray Micro-computed tomography of plants. *Microscopy and Microanalysis* 17, 2010–2011. doi:10.1002/jemt.20917.

Kachelrieß, M. (2008). Micro-ct. In *Molecular Imaging I* (pp. 23-52). Springer Berlin Heidelberg.

Kamenz, C., & Weidemann, G. (2009). Heavy metal—A contrasting substance for micro-tomographical visualization of scorpion book lungs. *Micron*, 40(8), 911-917. doi:10.1016/j.micron.2009.05.007

Kędzierski, M., Uchman, A., Sawlowicz, Z., & Briguglio, A. (2015). Fossilized bioelectric wire—the trace fossil *Trichichnus*. *Biogeosciences (Online)*, 12(8), 2301. doi:10.5194/bg-12-2301-2015

Kehlmaier, C., Dierick, M., & Skevington, J. H. (2014). Micro-CT studies of amber inclusions reveal internal genitalic features of big-headed flies, enabling a systematic placement of *Metanephrocera Aczél, 1948* (Insecta: Diptera: Pipunculidae). *Arth. Syst. Phylo*, 72, 23-36.

Keklikoglou, K., Chatzinikolaou, E., Faulwetter, S., Grigoriou, P., Papageorgiou, N., Queirós, A., Rühl, S., & Schmidbaur, H. (2015) Revealing effects of ocean acidification on the calcified structures of marine invertebrates through micro-computed tomography (micro-CT). *Bruker microCT 2015 user meeting, Belgium*.

Ketcham, R. A., & Carlson, W. D. (2001). Acquisition, optimization and interpretation of X-ray computed tomographic imagery: applications to the geosciences. *Computers & Geosciences*, 27(4), 381-400. doi:10.1016/S0098-3004(00)00116-3

Kim, J. S., Min, J., Recknagel, A. K., Riccio, M., & Butcher, J. T. (2011). Quantitative Three-Dimensional Analysis of Embryonic Chick Morphogenesis Via Microcomputed Tomography. *The Anatomical Record*, 294(1), 1-10. doi:10.1002/ar.21276

Kim, S. J., Xu, W., Ahmad, M. W., Baeck, J. S., Chang, Y., Bae, J. E., Chae K.S., Jeong T.K., Park J.A., Lee, G. H. (2016). Synthesis of nanoparticle CT contrast agents: in vitro and in vivo studies. *Science and Technology of Advanced Materials*, 16: 055003. doi:10.1088/1468-6996/16/5/055003

Knipfer, T., Eustis, A., Brodersen, C., Walker, A. M. & McElrone, A. J. (2015). Grapevine species from varied native habitats exhibit differences in embolism formation/repair associated with leaf gas exchange and root pressure. *Plant, Cell & Environment*, 38, 1503–1513. doi:10.1111/pce.12497

Kniss, J., Kindlmann, G., & Hansen, C. (2002). Multidimensional transfer functions for interactive volume rendering. *Visualization and Computer Graphics, IEEE Transactions on*, 8(3), 270-285. doi:10.1109/TVCG.2002.1021579

Koenigswald, W. V., Habersetzer, J., & Gingerich, P. D. (2011). Morphology and evolution of the distal phalanges in primates. *The World at the Time of Messel: Puzzles in Palaeobiology, Palaeoenvironment, and the History of Early Primates.*, 91-94.

Konietzko-Meier, D., & Schmitt, A. (2013). A histological study of a femur of *Plagiosuchus*, a Middle Triassic temnospondyl amphibian from southern Germany, using thin sections and micro-CT scanning. *Netherlands Journal of Geosciences*, 92(2-3), 97-108. doi:10.1017/S0016774600000020

Korte, N. & Porembski, S. (2011). Anatomical analysis of turgescient and semi-dry resurrection plants: the effect of sample preparation on the sample, resolution, and image quality of X-ray micro-computed tomography (μ CT). *Microscopy research and technique*, 74, 364–369. doi:10.1002/jemt.20917

Kuebler, K. E., McSween, H. Y., Carlson, W. D., & Hirsch, D. (1999). Sizes and masses of chondrules and metal-troilite grains in ordinary chondrites: possible implications for nebular sorting. *Icarus*, 141(1), 96-106. doi:10.1006/icar.1999.6161

Leroux, O., Leroux, F., Bellefroid, E., Claeys, M., Couvreur, M., Borgonie, G., Van Hoorebeke, L., Masschaele, B., Viane, R. (2009). A new preparation method to study fresh plant structures with X-ray computed tomography. *Journal of Microscopy*, 233, 1–4. doi:10.1111/j.1365-2818.2008.03088.x

Li, X., Pan, Z., Upadhyaya, S. K., Atungulu, G. G. & Delwiche, M. (2011). Three-dimensional geometric modeling of processing tomatoes. *Transactions of the American Society of Agricultural and Biological Engineers*, 54, 2287–2296. doi:10.13031/2013.40642

Lilje O, Lilje E, Marano A V, Gleason FH (2012) Three dimensional quantification of biological samples using micro-computer aided tomography (microCT). *Journal of microbiological methods* 92: 33–41. doi:10.1016/j.mimet.2012.10.006

Liu, Y., Scholtz, G., & Hou, X. (2015). When a 520 million-year-old Chengjiang fossil meets a modern micro-CT—a case study. *Scientific reports*, 5. doi:10.1038/srep12802

Lorensen, W. E., & Cline, H. E. (1987). Marching cubes: A high resolution 3D surface construction algorithm. In *ACM siggraph computer graphics*, 21(4), 163-169. doi:10.1145/37402.37422

McElrone, A. J., Choat, B., Parkinson, D. Y., MacDowell, A. A. & Brodersen, C. R. (2013). Using high resolution computed tomography to visualize the three dimensional structure and function of plant vasculature. *Journal of Visualized Experiments*, 74, e50162. doi:10.3791/50162

Meganck, J. A., Kozloff, K. M., Thornton, M. M., Broski, S. M., & Goldstein, S. A. (2009). Beam hardening artifacts in micro-computed tomography scanning can be reduced by X-ray beam filtration and the resulting images can be used to accurately measure BMD. *Bone*, 45(6), 1104-1116. doi:10.1016/j.bone.2009.07.078

Metscher, B. D. (2009a). MicroCT for comparative morphology: simple staining methods allow high-contrast 3D imaging of diverse non-mineralized animal tissues. *BMC physiology*, 9: 11. doi:10.1186/1472-6793-9-11

Metscher, B. D. (2009b). MicroCT for developmental biology: A versatile tool for high-contrast 3D imaging at histological resolutions. *Developmental Dynamics*, 238(3), 632-640. doi:10.1002/dvdy.21857

Metscher, B. D. (2011). X-ray microtomographic imaging of intact vertebrate embryos. *Cold Spring Harb Protoc*, 12, 1462-1471. doi:10.1101/pdb.prot067033

Meyer, M., Elliott, D., Wood, A. D., Polys, N. F., Colbert, M., Maisano, J. A., Vickers-Rich, P., Hall, M., Hoffman, K.H., Schneider, G., Xiao, S. (2014). Three-dimensional microCT analysis of the Ediacara fossil *Pteridinium simplex* sheds new light on its ecology and phylogenetic affinity. *Precambrian Research*, 249, 79-87. doi:10.1016/j.precamres.2014.04.013

Miller, J. S., & Venable, D. L. (2003). Floral morphometrics and the evolution of sexual dimorphism in *Lycium* (Solanaceae). *Evolution*, 57, 74–86. doi:10.1111/j.0014-3820.2003.tb00217.x

Mizutani, R., Takeuchi, A., Hara, T., Uesugi, K., & Suzuki, Y. (2007). Computed tomography imaging of the neuronal structure of *Drosophila* brain. *Journal of synchrotron radiation*, 14(3), 282-287. doi:10.1107/S0909049507009004

Mizutani, R., Takeuchi, A., Akamatsu, G., Uesugi, K., & Suzuki, Y. (2008a). Element-specific microtomographic imaging of *Drosophila* brain stained with high-Z probes. *Journal of synchrotron radiation*, 15(4), 374-377. doi:10.1107/S0909049508003725

Mizutani, R., Takeuchi, A., Uesugi, K., Takekoshi, S., Osamura, R. Y., & Suzuki, Y. (2008b). X-ray microtomographic imaging of three-dimensional structure of soft tissues. *Tissue Engineering Part C: Methods*, 14(4), 359-363.

Mizutani, R., Takeuchi, A., Uesugi, K., Takekoshi, S., Osamura, R. Y., & Suzuki, Y. (2009). Three-dimensional microstructural analysis of human brain tissue by using synchrotron radiation microtomographs. *Handbook on White Matter*, Nova Science Publishers, New York, 247-277.

Mizutani, R., & Suzuki, Y. (2012). X-ray microtomography in biology. *Micron*, 43(2), 104-115. doi:10.1016/j.micron.2011.10.002

Mooney, S. J., Pridmore T. P., Helliwell, J., Bennett, M. J. (2012). Developing X-ray computed tomography to non-invasively image 3-D root systems architecture in soil. *Plant and Soil*, 352, 1–22. doi:10.1007/s11104-011-1039-9

Needham, A. W., Abel, R. L., Tomkinson, T., & Grady, M. M. (2013). Martian subsurface fluid pathways and 3D mineralogy of the Nakhla meteorite. *Geochimica et Cosmochimica Acta*, 116, 96-110. doi:10.1016/j.gca.2012.07.004

Pajor, R., Fleming, A., Osborne, C. P., Rolfe, S. A., Sturrock, C. J. & Mooney, S. J. (2013). Seeing space: visualization and quantification of plant leaf structure using X-ray micro-computed tomography View Point. *Journal of Experimental Botany*, 64, 385–390. doi:10.1093/jxb/ers392

Paquit, V. C., Gleason, S. S. & Kalluri, U. C. (2011). Monitoring plant growth using high resolution micro-CT images. *Proceedings of SPIE-IS&T.*, 78770W–78770W–8. doi:10.1117/12.876719

Paredes, U. M., Prys-Jones, R., Adams, M., Groombridge, J., Kundu, S., Agapow, P. M., & Abel, R. L. (2012). Micro-CT X-rays do not fragment DNA in preserved bird skins. *Journal of Zoological Systematics and Evolutionary Research*, 50(3), 247-250. doi:10.1111/j.1439-0469.2012.00657.x

Paterson, G. L., Sykes, D., Faulwetter, S., Merk, R., Ahmed, F., Hawkins, L. E., Dinley, J., Bal, A.D., & Arvanitidis, C. (2014). The pros and cons of using micro-computed tomography in gross and micro-anatomical assessments of polychaetous annelids. *Mem Mus Victoria*, 71, 237-46.

Pauwels, E., Van Loo, D., Cornillie, P., Brabant, L., & Van Hoorebeke, L. (2013). An exploratory study of contrast agents for soft tissue visualization by means of high resolution X-ray computed tomography imaging. *Journal of microscopy*, 250(1), 21-31. doi:10.1111/jmi.12013

Penney, D., Dierick, M., Cnudde, V., Masschaele, B., Vlassenbroeck, J., Van Hoorebeke, L., & Jacobs, P. (2007). First fossil Micropholcommatidae (Araneae), imaged in Eocene Paris amber using X-ray computed tomography. *Zootaxa*, 1623, 47-53.

- Pierret, A., Capowiez, Y., Moran, C.J. & Kretzschmar, A. (1999). X-ray computed tomography to quantify tree rooting spatial distributions. *Geoderma*, 90, 307–326. doi:10.1016/S0016-7061(98)00136-0
- Pika-Biolzi, M., Hochuli, P. A., & Flisch, A. (2000). Industrial X-ray computed tomography applied to paleobotanical research. *Rivista Italiana Di Paleontologia E Stratigrafia*, 106(3), 369–377. doi:10.13130/2039-4942/6151
- Plougonven, E., Srichamnong, W., Srzednicki, G., Léonard, A. (2012) Characterisation of macadamia nuts using X-ray microtomography. *SkyScan microCT User meeting 2015, Belgium*.
- Presnell, J. K., Schreibman, M. P., & Humason, G. L. (1997). *Humason's animal tissue techniques*. Johns Hopkins University Press.
- Rahman, I. A., & Smith, S. Y. (2014). Virtual paleontology: computer-aided analysis of fossil form and function. *Journal of Paleontology*, 88(04), 633-635. doi:10.1666/13-0011
- Rivers, M. L., Sutton, S. R., & Eng, P. J. (1999). Geoscience applications of X-ray computed microtomography. In *SPIE's International Symposium on Optical Science, Engineering, and Instrumentation*. International Society for Optics and Photonics, 78-86.
- Roche, R. C., Abel, R. A., Johnson, K. G., & Perry, C. T. (2010). Quantification of porosity in *Acropora pulchra* (Brook 1891) using X-ray micro-computed tomography techniques. *Journal of Experimental Marine Biology and Ecology*, 396(1), 1-9. doi:10.1016/j.jembe.2010.10.006
- Rossi, M., Casali, F., Romani, D., Bondioli, L., Macchiarelli, R., & Rook, L. (2004). MicroCT Scan in paleobiology: application to the study of dental tissues. *Nuclear Instruments and Methods in Physics Research Section B: Beam Interactions with Materials and Atoms*, 213, 747-750. doi:10.1016/S0168-583X(03)01697-5
- Rowe, T., Kappelman, J., Carlson, W. D., Ketcham, R. A., & Denison, C. (1997). High-resolution computed tomography: a breakthrough technology for earth scientists. *Geotimes*, 42(9), 23-27.
- Ruthensteiner, B., Baeumler, N., & Barnes, D. G. (2010). Interactive 3D volume rendering in biomedical publications. *Micron*, 41(7), 886-e1. doi:10.1016/j.micron.2010.03.010
- Salmon, P. L., Liu, X., & Sasov, A. (2009). A post-scan method for correcting artefacts of slow geometry changes during micro-tomographic scans. *Journal of X-ray science and technology*, 17(2), 161-174. doi:10.3233/XST-2009-0220
- Sansone, S., Rocca-Serra, P., Field, D., Maguire, E., Taylor, C., Hofmann, O., Fang, H., Neumann, S., Tong, W., Amaral-Zettler, L., Begley, K., Booth, T., Bougueleret, L., Burns, G., Chapman, B., Clark, T., Coleman, L., Copeland, J., Das, S., Daruvar, Ad., Matos, Pd., Dix, I., Edmunds, S., Evelo, C. T., Forster, M. J., Gaudet, P., Gilbert, J., Goble, C., Griffin, J. L., Jacob, D., Kleinjans, J., Harland, L., Haug, K.,

Hermjakob, H., Sui, S. J. H., Laederach, A., Liang, S., Marshall, S., McGrath, A., Merrill, E., Reilly, D., Roux, M., Shamu, C. E., Shang, C. A., Steinbeck, C., Trefethen, A., Williams-Jones, B., Wolstencroft, K., Xenarios, I., & Hide, W. (2012). Toward interoperable bioscience data. *Nature Genetics* 44, 121-126. doi:10.1038/ng.1054

Schambach, S. J., Bag, S., Schilling, L., Groden, C., & Brockmann, M. A. (2010). Application of micro-CT in small animal imaging. *Methods*, 50(1), 2-13. doi:10.1016/j.ymeth.2009.08.007

Schmidbaur, H., Keklikoglou, K., Metscher, B. D., & Faulwetter, S. (2015). Exploring methods to remove iodine and phosphotungstic acid stains from zoological specimens. *Micro-CT User Meeting*. Bruges, Belgium, 116-123.

Simons, F. J., Verhelst F., & Swennen, R. (1997). Quantitative characterization of coal by means of microfocal X-ray computed microtomography (CMT) and color image analysis (CIA). *International journal of coal geology*, 34(1), 69-88. doi:10.1016/S0166-5162(97)00011-6

Staedler, Y. M., Masson, D. & Schönenberger, J. (2013). Plant Tissues in 3D via X-Ray Tomography: Simple Contrasting Methods Allow High Resolution Imaging. *PLoS ONE*, 8, e75295. doi:10.1371/journal.pone.0075295

Stanley, S. M. (1992). Exploring Earth and Life Through Time. *W H Freeman & Co, New York*.

Stuppy, W. H., Maisano, J. A., Colbert, M. W., Rudall, P. J., & Rowe, T. B. (2003). Three-dimensional analysis of plant structure using high-resolution X-ray computed tomography. *Trends in plant science*, 8(1), 2-6. doi:10.1016/S1360-1385(02)00004-3

Sutton, M. D., Briggs, D. E., Siveter, D. J., & Siveter, D. J. (2001). Methodologies for the visualization and reconstruction of three-dimensional fossils from the Silurian Herefordshire Lagerstätte. *Palaeontologia Electronica*, 4(1), 1-17.

Sutton, M. D. (2008). Tomographic techniques for the study of exceptionally preserved fossils. *Proceedings of the Royal Society of London B: Biological Sciences*, 275(1643), 1587-1593. doi:10.1098/rspb.2008.0263

Sutton, M., Rahman, I., & Garwood, R. (2013). *Techniques for virtual palaeontology*. John Wiley & Sons. 210 pp.

Tafforeau, P., Boistel, R., Boller, E., Bravin, A., Brunet, M., Chaimanee, Y., ... & Kay, R. F. (2006). Applications of X-ray synchrotron microtomography for non-destructive 3D studies of paleontological specimens. *Applied Physics A*, 83(2), 195-202. doi:10.1007/s00339-006-3507-2

Torrano-Silva, B. N., Ferreira, S. G., & Oliveira, M. C. (2015). Unveiling privacy: Advances in microtomography of coralline algae. *Micron*, 72, 34-38. doi:10.1016/j.micron.2015.02.004

- van der Niet, T., Zollikofer, C. P. E., de León, M. S. P., Johnson, S. D. & Linder, H. P. (2010). Three-dimensional geometric morphometrics for studying floral shape variation. *Trends in Plant Science*, 15, 423–426. doi:10.1016/j.tplants.2010.05.005
- Vodrážka R. (2009). A new method for the extraction of macrofossils from calcareous rocks using sulphuric acid. *Palaeontology*, 52(1), 187-192. doi:10.1111/j.1475-4983.2008.00829.x
- Wan, B., Xiao, S., Yuan, X., Chen, Z., Pang, K., Tang, Q., Guan, C., & Maisano, J. A. (2014). Orbisiana linearis from the early Ediacaran Lantian Formation of South China and its taphonomic and ecological implications. *Precambrian Research*, 255, 266-275. doi:10.1016/j.precamres.2014.09.028
- Wang, C. N., Hsu, H. C., Wang, C. C., Lee, T. K. & Kuo, Y. F. (2015). Quantifying floral shape variation in 3D using microcomputed tomography: A case study of a hybrid line between actinomorphic and zygomorphic flowers. *Frontiers in Plant Science*, 6, 724. doi:10.3389/fpls.2015.00724
- Wellington, S. L., & Vinegar, H.J. (1987). X-ray computerized tomography. *Journal of Petroleum Technology*, 39, 885–898.
- Yang, H., Chen, Z. Q., Wang, Y., Ou, W., Liao, W., & Mei, X. (2015). Palaeoecology of microconchids from microbialites near the Permian–Triassic boundary in South China. *Lethaia*, 48(4), 497-508. doi:10.1111/let.12122
- Zinsmeister, W. J., & De Nooyer, C. (1996). Computed tomography; non-destructive techniques for visualizing internal morphology of invertebrates. *Geological Society of America, Abstracts with Programs* 28 (7), 294.

7. Glossary of terms

3D	Three-dimensional
CCD camera	Charge-coupled device camera: a technology used in digital photography to convert a light signal into a digital value
Creative Commons licenses	A set of copyright-licenses that describe which rights of the licensed material are reserved and to what extent and under which condition the material can be modified and shared. The licenses are standardised, simple to understand and computer-readable (http://www.creativecommons.org).
CT	Computer tomography, a non-destructive imaging technique that converts projection views into orthogonal slices to calculate three-dimensional representations of the imaged object
CTVox	A commercial <u>volume rendering</u> software developed by SkyScan / Bruker
DICOM	Digital Imaging and Communications in Medicine: a standard providing format definitions and a communication protocol for the description and exchange of medical image data
DOI	Digital Object Identifier: a digital identifier used to uniquely identify an object and retrieve metadata about it. Mostly applied to documents such as scientific papers, books, reports, etc. but not restricted to these – any digital object can be assigned a DOI
Drishti	Free volume rendering software (http://sf.anu.edu.au/Vizlab/drishti)
Dryad / Datadryad	An online data repository to store data underlying scientific publications. Assigns DOIs to the submitted data so that they can be discovered and cited (http://datadryad.org).
figshare	An online data repository to store data underlying scientific publications. Assigns DOIs to the submitted data so that they can be discovered and cited (http://www.figshare.com)
GB	Gigabyte: 10 ⁹ bytes. A byte is a unit of digital information, its multiples

	(kilo-, mega-, gigabyte) are often used to describe the size of a digital storage medium, file or dataset.
GigaDB	An online data repository to store data underlying scientific publications, specializing on very large datasets. Assigns DOIs to the submitted data so that they can be discovered and cited (http://www.gigadb.org).
HMDS	Hexamethyldisilazane: a chemical used for drying specimens without affecting their morphology
ISA-TAB	A newly proposed data format intended to facilitate integration of diverse datasets across various life-science disciplines (http://www.isa-tools.org)
isosurface model	Geometrical, three-dimensional model consisting of surfaces of equal densities (often triangles)
keV	Kilo electron volt
kV	Kilovolt
metadata	Data about data. Ambiguous term, since data can be both “normal data” as well as “metadata”, depending on the context. Metadata help to understand the context of the data as well as provide a means to integrate it with other data.
μA	Micro-ampere
morphometric analysis	Statistical analysis based on the shape and size of morphological characters of organisms to detect similarities or significant differences between samples, populations or species
OBJ	Wavefront Object: a data format used to represent three-dimensional geometric objects with the information of color
pixel	The smallest unit of information in a digital image
projection image	Also called shadow image. Image that result from CT imaging, provide a grayscale side view of the specimen, with dense parts in darker shades and less dense parts in lighter shades of grey. From a series of projection images the cross-sections are calculated.
PTA	Phosphotungstic acid: an electron-dense stain used as a contrast agent in

	histology and CT imaging
RAM	Random-access memory: a form of computer data storage for fast access
reconstruction	Algorithmic process of transforming projection images into cross sections
ROI	Region of Interest: User-specified region of an image
SEM	Scanning Electron Microscopy: a high-resolution imaging technique
surface rendering, surface model	See isosurface model
transfer values, transfer function	In volume rendering, a definition of the colour and opacity values which with each voxel should be displayed
type material, type specimen	A biological reference specimen, usually kept in museums or biological collections, to which the scientific name of that specimen is formally attached
URI	Uniform Resource Identifier: a sequence of characters used to identify a web resource
URL	Uniform Resource Locator: often also synonymously used with “web address”, A URL is a URI which also provides a means to access the resource.
volume rendering	A way of displaying three-dimensional data acquired through 3D-imaging techniques such as CT or MRI. Depending on the transfer functions applied, different densities of the sample can be visualised and optionally colour-coded.
voxel	Volume pixel: the smallest unit of information in a three-dimensional digital space

8. Appendix

8.1 List of institutions with micro-CT

Table 8.1.1. Overview of the micro-CT labs hosted by the SYNTHESYS partners.

Micro-CT labs	Country	Micro-CT system	Further information
Natural History Museum in London	United Kingdom	Nikon Metrology HMX ST 225	http://www.nhm.ac.uk/our-science/departments-and-staff/core-research-labs/imaging-and-analysis-centre/nikon-metrology-hmx.html
Institute of Marine Biology and Genetics (HCMR)	Greece	Skyscan 1172	https://microct.portal.lifewatchgreece.eu/
Muséum National d'Histoire Naturelle (MNHN)	France	GE Phoenix VTomeX L240	http://ums2700.mnhn.fr/ast-rx/acces#tarification
Museo Nacional de Ciencias naturales (MNCN)	Spain	Nikon XT-H-160	http://www.mncn.csic.es/index.jsp?seccion=1325&id=2010120902260001&activo=12
Wageningen University and Research Centre	Netherlands	GE Phoenix v[tome]x m	http://www.wageningenur.nl/en/Expertise-Services/Facilities/CATAgroFood-3/CATAgroFood-3/Our-facilities/Show/Xray-computer-Tomography-XRT-CT-Noninvasive-3D-imaging-of-internal-structures.htm
Naturalis Biodiversity Center	Netherlands	Skyscan 1172	https://science.naturalis.nl/en/labs-services/laboratories/geolab/
Národní Museum	Czech Republic	Skyscan 1172	http://www.nm.cz/

Museum für Naturkunde	Germany	Phoenix Nanotome s	https://muellerlaboratory.wordpress.com/ https://www.kristin-mahlow.de/mico-ct-labor/
-----------------------	---------	----------------------	--

Table 8.1.2. Indicative list of micro-CT labs all over the world

Micro-CT labs	Country	Micro-CT system	Further information
Henry Moseley X-ray imaging facility, University of Manchester	United Kingdom	E.g. Nikon Metrology 225/320 kV Nikon XTH 225	http://www.mxif.manchester.ac.uk/resources/imaging-systems/
The Musculoskeletal Imaging Core at UMASS Medical School	USA	Scanco MicroCT40	http://www.umassmed.edu/orthopedics/research/musculoskeletal-imaging/
CNS - Center for Nanoscale Systems	USA	Nikon Metrology HMX ST 225	http://cns.fas.harvard.edu/microCT
Rush University Medical Center - microCT Core Lab	USA	Scanco MicroCT40 Scanco MicroCT50	https://www.rushu.rush.edu/servlet/Satellite?c=RushUnivLevel3Page&cid=1235357858244&pagename=Rush%2FRushUnivLevel3Page%2FLevel_3_Audience_Portal_Page
University of Minnesota XRCT lab	USA	X-View CT X5000	http://xraylab.esci.umn.edu/
High-Resolution X-ray Computed Tomography Facility at the University of Texas at Austin (UTCT)	USA	Xradia microXCT 400 NSI scanner	http://www.ctlab.geo.utexas.edu/
University of Mississippi Medical Center Department of Biomedical Materials Science	USA	Skyscan 1172	https://www.umc.edu/sod/
Centre for X-ray Tomography of the Ghent University (UGCT)	Belgium	NanoWood Environmental Micro-CT Medusa	http://www.ugct.ugent.be/
Institute for Biomechanics - ETH Zürich	Switzerland	Scanco μ CT 41, 50 and 80	http://www.biomech.ethz.ch/

SYNTHESYS3 - Best practice for micro-CT

Mario Negri Institute of Milan	Italy	GE Explore Locus	http://www.marionegri.it/en_US/home
Weizmann Institute of Science	Israel	Xradia microXCT 400	http://www.weizmann.ac.il
Stellenbosch University CT Scanner Unit	South Africa	GE Phoenix VTomeX L240	http://academic.sun.ac.za/saf/
Aix-Marseille Université (AMU), Laboratoire Cerege	France	MicroXCT-400 Zeiss-Xradia	http://nano-id.fr/Tomographie-RX
De la Préhistoire à l' Actuel: Culture, Environment, Anthropologie (PACEA)	France	GE Phoenix VTomeX	http://www.pacea.u-bordeaux1.fr/
Laboratoire Biogéosciences, University of Bourgogne	France	SkyScan 1174	http://biogeosciences.u-bourgogne.fr/en/
Institut de Paléoprimatologie, Paléontologie Humaine: Evolution et Paléoenvironnements (IPHEP), Université de Poitiers	France	RX solutions EasyTom XL Duo Viscom X8050	http://iphep.labo.univ-poitiers.fr/index.php/fr/ http://sfa.univ-poitiers.fr/imageup/equipements/microtomographie/
Structure Fédérative de Recherche de Lyon Gerland (SFR), BioSciences	France	GE Phoenix Nanotom S	http://www.sfr-biosciences.fr/ http://www.sfr-biosciences.fr/plateformes/Phenotypage-cellulaire/AniRA-ImmOs/AniRA-immos
Laboratoire IPANEMA	France	PSICHÉ METROLOGIE ANATOMIX	http://www.synchrotron-soleil.fr/Recherche/LignesLumiere/PSICHE http://www.synchrotron-soleil.fr/Recherche/LignesLumiere/METROLOGIE http://ipanema.cnrs.fr/spip/
Theoretical Biology MicroCT Imaging Lab, University of Vienna	Austria	MicroXCT-200 Zeiss-Xradia Skyscan 1174	https://theoretical.univie.ac.at/microct-lab/
Vienna Micro-CT Lab, Department of Anthropology	Austria	Viscom X8060	http://www.micro-ct.at/en/

Department of Palaeontology, University of Vienna	Austria	Skyscan 1173	http://www.univie.ac.at/Palaeontologie/FACILITIES2_DE.html
Institute of Biotechnology, Cornell University	USA	Xradia Zeiss VersaXRM-520 GE eXplore CT-120	http://www.biotech.cornell.edu/node/573

8.2 List of microCT manufacturers

Table 8.2.1. MicroCT manufacturers and their company links (modified table from Schambach et al. 2010 and <http://microctworld.net/>)

Company	Website
<i>Bruker (acquisition of Skyscan and Carestream)</i>	http://bruker-microct.com/home.htm http://www.carestream.com/default.aspx?LangType=1033
<i>CT imaging</i>	http://www.ct-imaging.de/en/
<i>Echo Medical Systems</i>	http://www.echomri.com/
<i>FEI</i>	http://www.fei.com/
<i>GE Medical Systems</i>	http://www.gehealthcare.com
<i>GE Measurement and Control Solutions</i>	http://www.ge-mcs.com/index.php
<i>Hitachi Aloka Medical</i>	http://www.hitachi-aloka.co.jp/english/
<i>Mediso</i>	http://www.mediso.hu/
<i>Milabs</i>	http://www.milabs.com/
<i>NanoFocus Ray</i>	http://www.nfr.kr/e_index.php
<i>Nikon Metrology</i>	http://www.nikonmetrology.com/en_EU/
<i>North Star Imaging (XviewCT)</i>	http://www.xviewct.com/
<i>Perkin Elmer</i>	http://www.perkinelmer.com/
<i>Prexion</i>	http://www.prexion.com/
<i>RX Solutions</i>	http://www.rxsolutions.fr/
<i>Scanco Medical</i>	http://www.scanco.ch/

<i>Sedecal</i>	http://www.sedecal.com/sedecal.com/es/home/index.php?i=1
<i>Siemens</i>	http://www.siemens.com/entry/cc/en/
<i>Stratec Medizintechnik GmbH</i>	http://www.stratec-med.com
<i>Toshiba IT & Control Systems Corporation</i>	http://www.toshiba-itc.com/en/index.html
<i>TriFoil imaging (acquisition of Bioscan Inc.)</i>	http://www.trifoilimaging.com/
<i>Varian Medical Systems</i>	https://www.varian.com
<i>Werth Messtechnik</i>	http://www.werth.de/de/start/home.html
<i>Xstrahl</i>	http://www.xstrahl.com/
<i>YXLON International GmbH</i>	http://www.yxlon.com/
<i>Zeiss</i>	http://www.xradia.com/

8.3 List of softwares

Table 8.3.1. 3D Volume Rendering softwares (modified table from Walter et al. (2010) and Abel et al. (2012))

Software	Licence Type	URL
VG Studio Max	Commercial	www.volumegraphics.com
SPIERS	Free	www.spiers-software.org
DRISHTI	Free	www.sf.anu.edu.au/Vizlab/drishti/
ImageJ	Free	www.rsb.info.nih.gov/ij/
Mimics	Commercial	www.materialise.com/mimics
Simpleware	Commercial	www.simpleware.com
Amira	Commercial	www.amira.com
Blender	Free	www.blender.org
Arivis (web-based software)	Commercial	http://vision.arivis.com/
tomviz	Free	http://www.tomviz.org/
BioImageXD	Free	http://www.bioimagexd.net

Fiji	Free	http://fiji.sc/3D_Viewer
Imaris	Commercial	http://www.bitplane.com/
Huygens	Commercial	http://www.svi.nl
Image-Pro	Commercial	http://www.mediacy.com
Volocity	Commercial	http://www.improvision.com
VTK	Free	http://www.vtk.org/
Slice:Drop (web-based software)	Free	http://slicedrop.com/
Voluminous (web-based software)	Free	http://voluminous.nci.org.au/
Brain Maps (web-based software)	Free	http://brainmaps.org
CTVox	Free	http://bruker-microct.com/products/ctvox.htm
Open Inventor	Commercial	http://www.openinventor.com/

Table 8.3.2. Softwares for 2D visualisation (modified table from Walter et al. (2010) and Abel et al. (2012))

Software	Licence Type	URL
VG Studio Max	Commercial	www.volumegraphics.com
SPIERS	Free	www.spiers-software.org
ImageJ	Free	www.rsb.info.nih.gov/ij/
Mimics	Commercial	www.materialise.com/mimics
Simpleware	Commercial	www.simpleware.com
Amira	Commercial	www.amira.com
Arivis (web-based software)	Commercial	http://vision.arivis.com/

tomviz	Free	http://www.tomviz.org/
BioImageXD	Free	http://www.bioimagexd.net
Fiji	Free	http://fiji.sc/3D_Viewer
Imaris	Commercial	http://www.bitplane.com/
Huygens	Commercial	http://www.svi.nl
Image-Pro	Commercial	http://www.mediacy.com
Volocity	Commercial	http://www.improvision.com
VTK	Free	http://www.vtk.org/
Slice:Drop (web-based software)	Free	http://slicedrop.com/
Brain Maps (web-based software)	Free	http://brainmaps.org

Table 8.3.3. Segmentation softwares (modified table from Walter et al. (2010) and Abel et al. (2012))

Software	Licence Type	URL
VG Studio Max	Commercial	www.volumegraphics.com
SPIERS	Free	www.spiers-software.org
DRISHTI	Free	www.sf.anu.edu.au/Vizlab/drishti/
Mimics	Commercial	www.materialise.com/mimics
Simpleware	Commercial	www.simpleware.com
Amira	Commercial	www.amira.com
BioImageXD	Free	http://www.bioimagexd.net

Table 8.3.4. 2D/3D analysis softwares (modified table from Walter et al. (2010) and Abel et al. (2012))

Software	Licence Type	URL
VG Studio Max	Commercial	www.volumegraphics.com
ImageJ	Free	www.rsbi.info.nih.gov/ij/
Simpleware	Commercial	www.simpleware.com
Amira	Commercial	www.amira.com
Stratovan Checkpoint	Commercial	www.stratovan.com
Meshlab	Commercial	www.meshlab.sourceforge.net/
Arivis (web-based software)	Commercial	http://vision.arivis.com/
tomviz	Free	http://www.tomviz.org/
BioImageXD	Free	http://www.bioimagexd.net
Fiji	Free	http://fiji.sc/3D_View
Imaris	Commercial	http://www.bitplane.com/
Huygens	Commercial	http://www.svi.nl
Image-Pro	Commercial	http://www.mediacy.com
Volocity	Commercial	http://www.improvision.com
VTK	Free	http://www.vtk.org/